Joint Programming Initiative on Cultural Heritage and Global Change

HERITAGE PLUS Call

PROTHEGO

Protection of European Cultural Heritage from Geo - Hazards

JPI-CH Heritage Plus collaborative research project [2015-2018]

Document Reference

WP6: Local scale investigation and advanced modelling

Deliverables: D.05.02

Local scale investigation and advanced modelling of the geo-hazards affecting the Derwent Valley Mills World Heritage Case Study Site

Version 1.0

Date of Issue: 12/09/2018

Author(s):	Harrison, A.M., Novellino, A., Hobbs, P.R.N., Wang, L & Bee, E. [British Geological Survey]	28/02/2018
Reviewed by:	Daniele Spizzichino [ISPRA]	31/08/2018
Approved by:	Claudio Margottini [ISPRA]	12/09/2018

Dissemination Level: PU (Public)

How to cite this document

HARRISON, A.M., NOVELLINO, A., HOBBS, P.R.N., WANG, L & BEE, E. (2018). *PROTHEGO Deliverable D.05.02* Local scale investigation and advanced modelling of the geo-hazards affecting the Derwent Valley Mills World Heritage Case Study Site, Version 1.0. JPI-CH Heritage Plus PROTHEGO project, Open Report. Date 12/09/2018. pp. Page(s) 38. Available at: www.prothego.eu

Acknowledgements

In addition to the Authors, Reviewer(s) and Approver of this report who are acknowledged in the front page, a number of staff from the Project Partners organisations (ISPRA, NERC, CUT, UNIMIB and IGME) contributed to the development of the work described in this report, both during the design and the lifetime of the project. Of the many individuals who have contributed to this work, the author(s) would particularly like to thank Adam Lathbury (Head of Derbyshire County Council's Conservation, Heritage and Design Service) and Adrian Farmer (DVMWHS Heritage Co-ordinator) for their huge background knowledge and input regarding their needs and requirements when managing the Derwent Valley Mills WHS.

Revision history

Revision	Date	Author(s)	Description
1.0	12/09/2018	HARRISON, AM	PROTHEGO partners external review

Executive summary

PROTHEGO (**PROT**ection of European Cultural **HE**ritage from **G**e**O**-hazards) is a collaborative research project funded in the framework of the Joint Programming Initiative on Cultural Heritage and Global Change (JPICH) – Heritage Plus in 2015–2018. The aim of the PROTHEGO project is to develop and validate an innovative multi-scale methodology for the detection and monitoring of European Cultural Heritages exposed to natural hazards.

Work Package 5 (WP5) focussed on the local-scale assessing, monitoring and modelling of geohazards affecting the Derwent Valley, one of the World Heritage List (WHL) site selected during WP4 (D04.02) The analysis conducted used in-situ observation, Interferometric Synthetic Aperture Radar (InSAR) results and flooding simulations based on different climate change scenarios in order to validate the impact of the natural hazards in the Derwent Valley catchment area. The results show that two landslides, in Starkholmes and Ambergate, and flooding, mainly over the west river bank, are the main geohazards affecting the site with the possibility to experience increased geohazards in the coming decades due to changes in climate.

Table of contents

1 Introduction

The Derwent Valley and its associated mills is an example of one of the key sites of Britain's industrial revolution (18th century). It was included in the UNESCO World Heritage List in 2001 due to its international role in the birth of the modern factory system, the development of new technology for spinning cotton and the first modern industrial settlements, e.g. Cromford, Belper and Milford [5] (UNESCO Ref. 1030; WHL inscription criteria: ii and iv [6]).

The Derwent Valley Mills World Heritage Site (DVMWHS) comprises a largely rural, industrial landscape with a number of historic cotton and silk mill complexes (e.g. Strutt's North Mills and East Mills, Masson Mills, Cromford Mills, Darley Abbey Mills and Derby Silk Mill), the watercourses that powered them, railways, housing settlements and other facilities developed for the mill-worker communities during the 18th and 19th centuries.

The Derwent Valley encompasses a c.24 km long stretch of the lower course of the Derwent river valley, from Derby in the south to Matlock Bath in the north where it almost abuts the southern boundary of the Peak District National Park (Figure 1a).

UNESCO has outlined and divided the DVMWHS into the Core Area and the Buffer Zone. The Core Zone is a single entity (12.29 km^2 extended), encompassing historic buildings, features and landscapes and excluding detailed elements, linked by linear features where these were the defining characteristic of the historic topography and contributed to the universal value of the site. The outlined boundary, wherever possible, coincided with existing statutory and formal designations within administrative areas where relevant to the inscription criteria, and tests of authenticity were applied in relation to the historical evolution of the cultural landscape.

The Buffer zone aims to protect the WHS from negative influences. It represents a zone, that in itself is not of outstanding universal value, but that may influence the World Heritage site (UNESCO, 2009). The Buffer Zone therefore embraces the Core Area in order to protect the site from any development which would damage it. Geographically the DVMWHS buffer zone extends for 43.63 km^2 across the nearby countryside, also following and being defined in some areas by the topography of the steep sides of the river valley (Figure 1a).

The DVMWHS Core Area and Buffer Zone are characterised by undulating topography with elevations ranging between 45 m OD in the south of the area to 325 m OD, in the north (Figure 2a). A deeply incised gorge at Matlock Bath (SK 2931 5823), in the north of the DVMWHS, and a relatively narrow valley floor to the south towards the confluence with the River Trent define the topography suitable for the development and installation of water-powered spinning mills in the 18th and 19th centuries. The power of the River Derwent is still exploited at a number of these historic mill sites, producing hydro-electricity from turbines instead.

The heritage assets within the UNESCO site are protected through a variety of UK planning and conservation laws, and since 2010 the site is managed by the DVMWHS Management Board, a locally-based partnership funded by the Local Authorities, predominantly Derbyshire County Council.

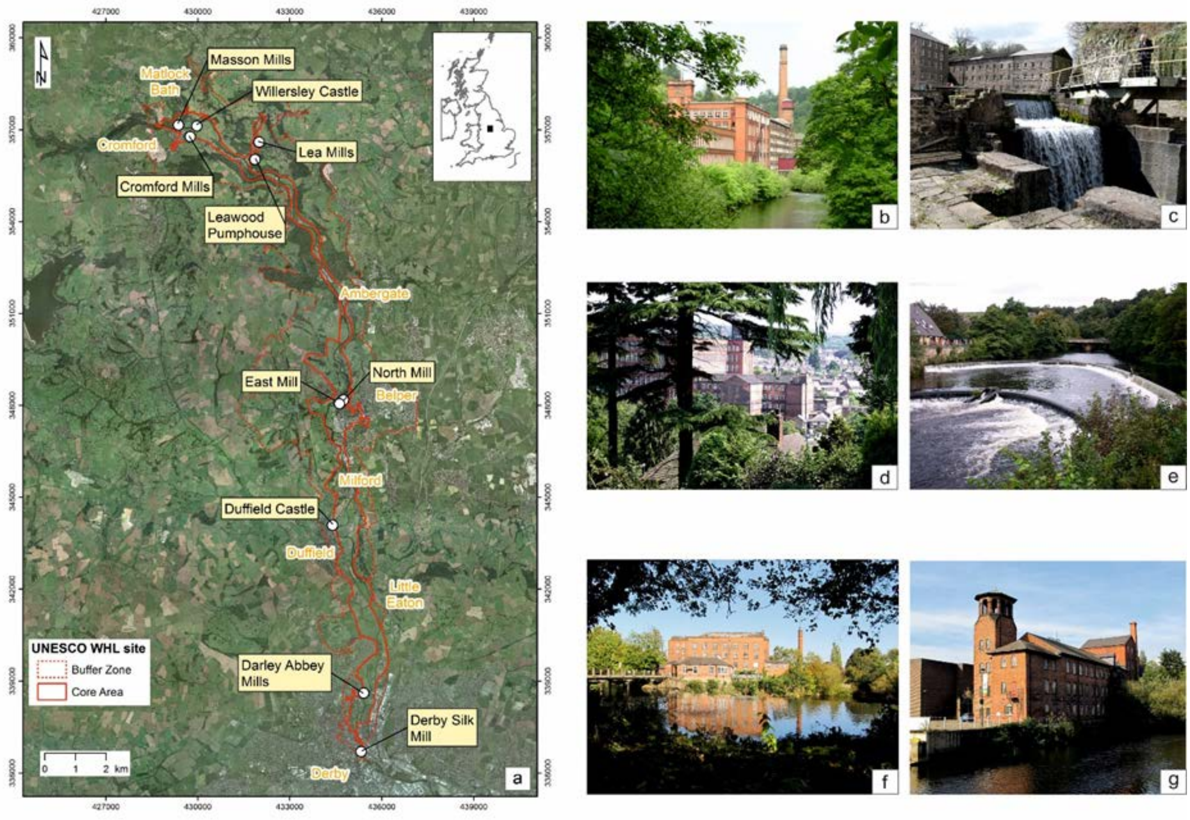

Figure 1. Core Area and Buffer Zone boundaries of the Derwent Valley Mills UNESCO WHL site with indication of key World Heritage buildings and mill complexes, overlapped onto aerial photography (a). Photographs of: Masson Mills (b), Cromford Mills (c), North and East Mill in Belper (d), River Derwent in Milford (e) Darley Abbey Mills (f) and Derby Silk Mill (g). Map units: British National Grid; projection: Transverse Mercator; datum: OSGB 1936. WHL site boundaries © Historic England 2015; Contains Ordnance Survey data © Crown copyright and database right 2015.

The site also includes contemporary infrastructure, principally railways, roads and canals, situated in the valley floor and in some cases on the valley sides. Quarries were also an important part of the site, and the Derbyshire Dales generally, providing the raw materials for the rapid increase in construction during the 18th and 19th centuries. Key to these developments was their scale, in terms of buildings, workforce and transport, in comparison to previous small-scale rural practice. Due to the relocation of industry to Lancashire during the 19th Century, the infrastructure remained in the original condition and has only more recently been renovated for new uses. Therefore, the identification of areas exposed to potential geohazard risks and their evolution in time can offer crucial information for decision makers, to aid mitigation and planning to protect the cultural and heritage site and surrounding landscapes from natural hazards.

This report is structured as follows: firstly the geological setting is introduced in section 2; a summary of the main geohazards present in the DVMWHS in provided in section 3. Section 4 provides both the large and local scale ground motion monitoring results from spaceborne imagery. Section 5 models the landslide, subsidence and flooding susceptibilities, identified and monitored in Section 3 and 4, considering UKCP09 climate projections. Section 6 discusses the main findings and, section 7 presents the proposed mitigation measures and finally the conclusions are described in section 8.

2 Geological context

The DVMWHS is overlain by sporadic Quaternary superficial deposits, which are mostly located within the Core Zone. These deposits mainly consist of Alluvium, (fluvial deposits found in the valley bottom covering much of the Core Zone as it follows the River Derwent's path). Head deposits (draped on some of the valley sides, with origins upslope and forming due to solifluction, soil creep and hillwash). A small number of river terraces have been mapped, close to the current river position, once the river floodplain, erosion has cut down to the river in its present day location. These superficial deposits consist of clay, silt, sand and gravel, depending on their origin and depositional environment. Towards the edges of the Buffer Zone, patches of glacially-derived till deposits have been mapped. These are diamictons made up of a range of particle sizes.

The underlying bedrock geology predominantly consists of thick interbedded mudstone, siltstone and sandstone of the Carboniferous Millstone Grit Group (358.9 to 398.9 Mya) through much of the central part of the DVMWHS area (Figure 2b). The oldest rocks in the area are Lower Carboniferous in age (limestone with sandstone and mudstones) and only outcrop in the northernmost part of the site around Matlock Bath and Cromford. These are overlain by the Bowland High and Craven Groups (Mississippian), with small outcrops in both the northern and southern parts of the site. Within the interbedded mudstones, siltstones and sandstones of the Bowland High and Craven Groups, alternating permeable and impermeable rocks can frequently give rise to landslide susceptibility, especially so if the river undercuts the toe of the steep-sided slopes (see section 4). Younger Triassic rocks (mudstone, siltstone and sandstones) are found underlying the flatter, southernmost part of the site, around Derby.

Over the last two centuries most of the industrial landscape and complexes have been well-preserved and the upper reaches of the valley are still intact, however, present and future environmental and geological processes could expose these heritage assets to a series of threats, including surface water and fluvial flooding, contaminated sediment transport and remobilisation of deposits/minerals historic mining activities (Howard et al., 2015).

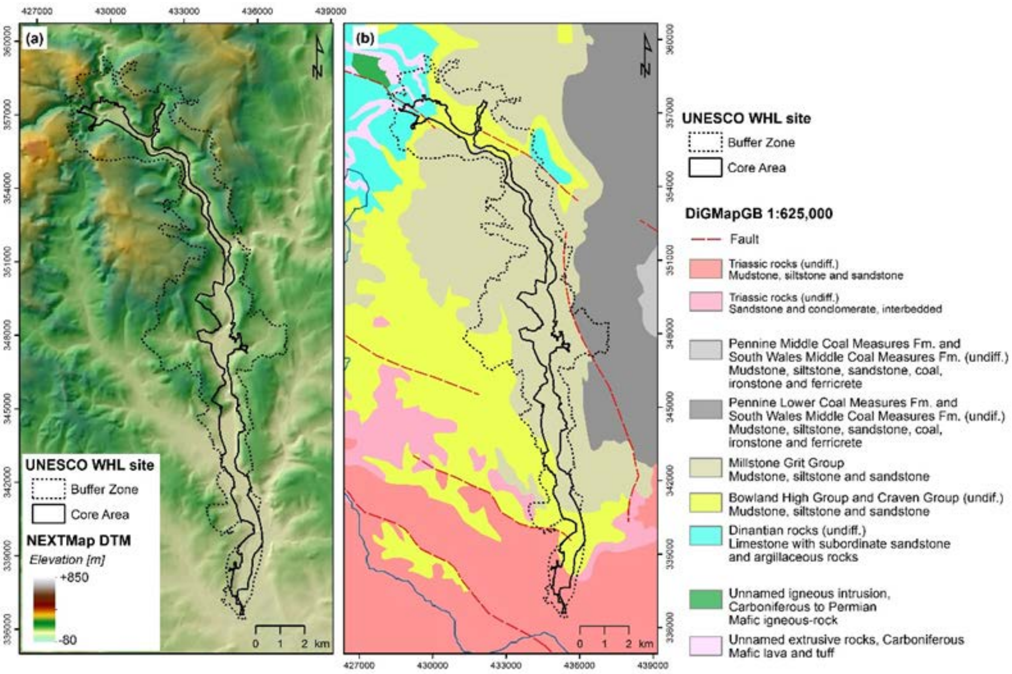

Figure 2. Derwent Valley Mills UNESCO WHL site boundaries overlapped onto: (a) NEXTMap digital terrain model and shaded relief at 10 m resolution; and (b) bedrock geology from BGS DiGMapGB at 1:625,000 scale. Map units: British National Grid; projection: Transverse Mercator; datum: OSGB 1936. WHL site boundaries © Historic England 2015; Contains Ordnance Survey data © Crown copyright and database right 2015; NEXTMap® Britain elevation data © Intermap Technologies; Geological materials © NERC. All rights reserved.

3 Geo-hazard context

In order to assess the susceptibility of natural geohazards affecting DVMWHS the analysis of the following datasets has been considered:

1. BGS Geosure, a dataset (based on geological and geotechnical factors) which classifies natural ground stability susceptibility to geohazards at 1:50,000 scale (Booth et al., 2010). These geohazards include collapsible deposits, compressible ground, debris flow, landslides, running sands, shrink-swell, and soluble rocks. Each hazard is rated using a straightforward A to E classification representing increasing hazard.
2. BGS National Landslide Database (NLD), a point-database where each landslide is identified by an ID number and a point location, (usually taken as the landslide backscarp feature), (Foster et al., 2012). Each landslide is also documented with information on name, size, dimensions, typology, trigger, damage caused, movement date, age and a bibliographic reference where available.
3. Geological Indicators of Flooding (GIF) (Booth et al., 2010) and Susceptibility to Groundwater Flooding (BGS, 2016) are two datasets that assess the potential for fluvial and groundwater flooding.
4. Interferometric Synthetic Aperture Radar (InSAR) results for the monitoring of the spatio-temporal ground deformation, available for the period 2015-2017.
5. High-resolution digital elevation models from Light Detection And Ranging (LiDAR) data for mapping, monitoring and modelling mass movements. LiDAR has been provided for 2014 and 2016 by the Environment Agency (EA) and generated at spatial resolutions of between 25cm and 2 m.
6. Soil and Land-use based rainfall-runoff-recharge Model (SLiM), a BGS developed soil moisture balance model to simulate runoff and potential groundwater recharge processes using spatio-temporal weather and catchment characteristics under the climate change UKCP09 projection for gas emission scenarios.

It is important to not only assess the present day geohazard risks to DVMWHS, but also to look to the future and consider the effects of climate change on the area and how this might effect geohazard susceptibility. GeoSure, the NLD and InSAR informed an assessment of the current geological factors in the area. SLiM has been applied to build a forecast scenario model of the impacts of climate change on ground instability and flooding conditions based on UKCP09 climate projections.

3.1 DVMWHS Geohazards

All 7 GeoSure geohazard datasets have been analysed individually to assess their spatial distribution against the official boundaries of the DVMWHS (Figure 3) and assess the proximity to various key heritage locations/assets. The results and descriptions about each hazard are provided below.

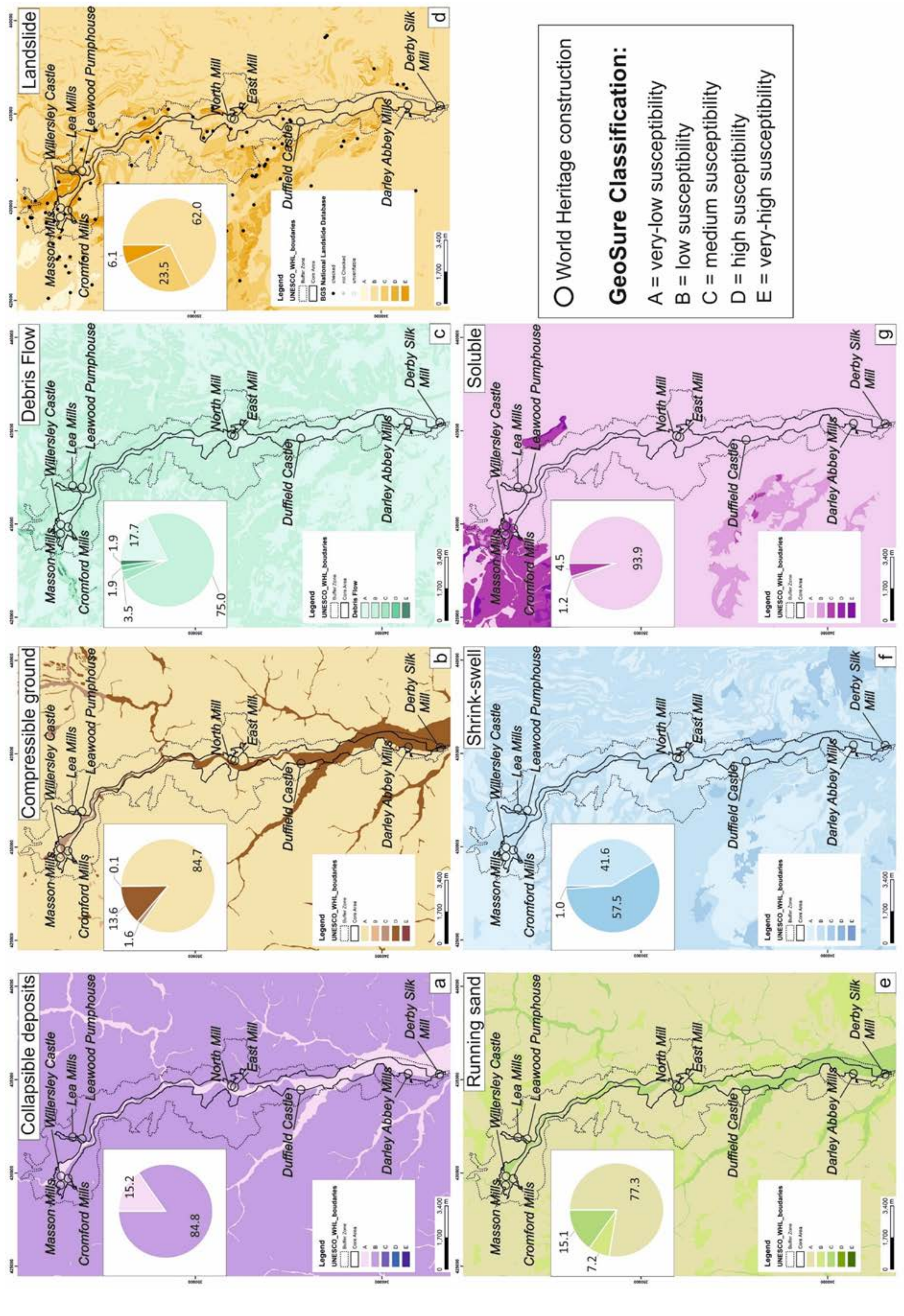

Figure 3. Potential hazards in the DVMWHS combined buffer and core zones associated with collapsible deposits (a), compressible ground (b), debris flow (c), landslide (d), running sand (e), shrink-swell terrain (f) and soluble rocks (g). Location of key World Heritage buildings and mill complexes is shown. Based upon Geosure dataset, with the permission of the British Geological Survey.

3.1.1 Collapsible deposits

Collapsible deposits refer to material which can collapse when saturated or when a load, such as a building or road traffic, is placed on them. Figure 3a shows the results of the analysis for collapsible deposit base on BGS GeoSure dataset. The area has a predominantly low susceptibility with B rating amounting to 84.8% of the DVMWHS site and a limited section (15.2%), confined to the Derwent river deposits with a very-low susceptibility (Figure 3a).

3.1.2 Compressible ground

Compressible ground contains layers of very soft materials, such as clay or peat that may compress if loaded by overlying structures or as a consequence of groundwater level changes potentially resulting in depression of the ground and disturbance of foundations.

The very-high (E) susceptibility is associated with clay and silt alluvium river deposits in the southernmost part of the DVMWHS buffer encompassing Duffield Castle, Darley Abbey Mills and Derby Silk Mill while 84.7% of the area belong to the very-low susceptibility (Figure 3b). Nevertheless, compressible ground does not appear to be of particular concern for the conservation of tangible cultural asset (see Section 4.2).

3.1.3 Debris Flow

The Debris Flow landslide layer provides information on the potential of the ground, at a given location, to form a debris flow. Debris flows are rapid, downslope flow of poorly sorted debris mixed with water. They are a widespread phenomenon in mountainous terrain and are distinct from other types of landslides as they can occur periodically on established paths, usually gullies and drainage channels. Debris Flow susceptibility is based on a combination of geological, hydrogeological and topographic data. The methodology develops an additional dimension to the BGS GeoSure landslides layer (see Section 3.1.4).

The very-high susceptibility is concentrated in the northern sector, nearby Matlock Bath and Cromford, where gullies and first- or second-order drainage channels can develop along the outcrops of Carboniferous extrusive rocks and Millstone Grit Group (see Figure 2b). However, none of the World Heritage site, according to the data available, is susceptible to debris flow hazard (Figure 3c).

3.1.4 Landslide

The GeoSure Landslide layer considers all downslope movement of rock, debris or earth under gravity except debris flow (Gibson et al. 2013). The susceptibility is evaluated from geology, geotechnics and slope angle. The geology, topography and climate of the Derwent Valley have lent themselves to the development of landslides in the past, mostly having natural origins in the Ice Age, the great majority of these are relic features and are not active at the present time. When re-activation occurs it usually affects only a part of the relic landslide and may not exhibit the original mechanism. Up to date, the BGS NLD reports 44 landslides, 13 of them within the Core Area, which correspond to the highest landslide susceptibility in GeoSure (see Figure 3d). They are mostly rotational to shallow flow types which range in size from 0.02 to 1.00 km^2 with the greatest concentration in the northern half (Figure 4a). Their re-activation has already generated disruption for road and rail construction, mining, quarrying, housing development and drainage.

At the same time not all landslides events are recorded, especially landslide types such as rockfalls which can occur in the DVMWHS. These develop on the steep crags and scarps where bedrock is exposed to the elements, typically at or near the crest of the slope (Figure 4b). Other landslide types that are unlikely to be recorded in the NLD are small mudflows that may go unnoticed and are ephemeral in a rural (wooded or farmed) setting; becoming rapidly degraded. Of course, this applies equally to other shallow landslide types where they are situated away from habitation, infrastructure or farming (Figure 4c).

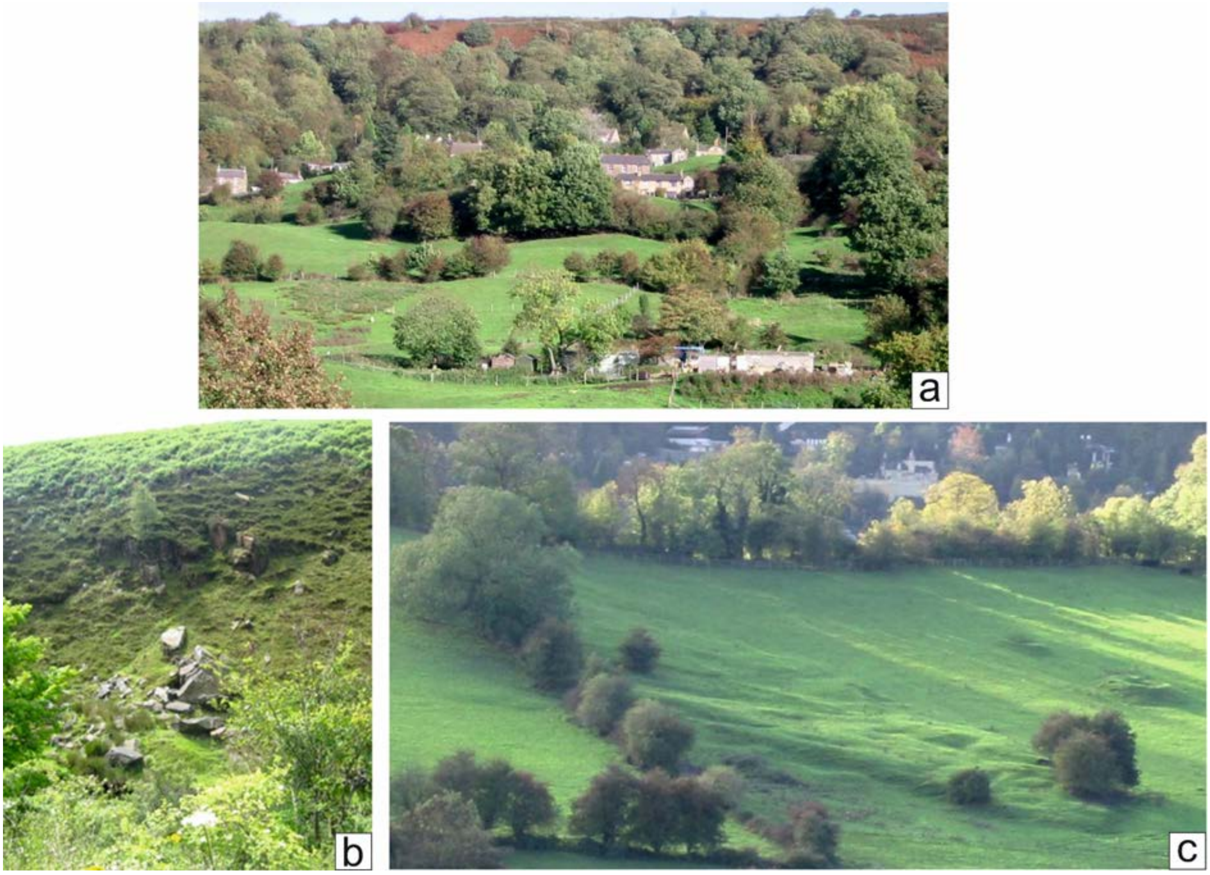

Figure 4. Some of the landslides in the DVMWHS: rotational landslide blocks at Starkholmes (a), Fresh rockfall from a crag in Millstone Grit Series (b) and shallow landslide near Station Quarry, Matlock (c). Modified from Pennington et al. (2009).

Landslides in DVMWHS are generally tree-covered and often intimately associated with quarrying activities (e.g. stone extraction from backscarps) and have not been surveyed. Consequently, it is also likely that in some cases their full extent has not been captured in the original mapping. A few landslides occur in head and till deposits, though it's worth noting that this deposit is not comprehensively mapped in Britain and may be involved in other landslides within the DVMWHS, principally shallow landslides within which head can play a key role (Pennington et al., 2009).

Spatial distribution of the largest landslides have been a critical factor in the selection of the best SAR acquisition geometry (see Section 4.2).

3.1.5 Running Sand

Some types of ground, can contain loosely packed sandy layers that can become fluidized by water flowing through them. Such sands can 'run' and remove support from overlying buildings and cause potential damage. Due to the absence of excavations in sand deposits below the water table and the absence of springs occurrence at the base of sand outcrops and given the low seismicity of the area, the largest portion (77.3%) of DVMWHS extension is ascribed to category A (Figure 3e).

3.1.6 Shrink-swell

Clay-rich deposits can change volume due to variations in moisture (water content), this shrinking and swelling might cause ground movement particularly in the upper 2 m and affect foundations, pipes and services. A medium shrink-swell susceptibility is attributed to alluvial and mass movement deposits along the river Derwent (Figure 3f), however the majority of the site has a low shrink-swell potential.

3.1.7 Soluble rock

Some types of ground, contain layers of material that can be dissolved by water. This can cause underground cavities to develop. These cavities reduce support to the ground above and can lead to a collapse of overlying material (Farrant and Cooper 2008; Cooper et al. 2011).

The highest levels (C and D) of soluble rock susceptibility, despite representing 5.7% of the DVMWHS area are concentrated in the northern sector where bedrock geology is represented by Carboniferous extrusive rocks and Dinantian Limestone still quarried today in Cromford (see Figure 2b). This sector contains Masson Mills, Cromford Mills and Willersley Castle sites (Figure 3g).

3.1.8 Flooding

Flooding from rivers is controlled by antecedent soil moisture capacities and rainfall intensities and durations. Whilst villages and towns for the mill workers are situated on higher terraces along the valley sides within sectors susceptible to landslide in the Buffer Zone (which does not show a high susceptibility to fluvial flooding), in the Core Area, the mills and the infrastructure are adjacent to the river making them particularly susceptible to erosion and fluvial flooding as a result of high flow rates associated with high intensity rainfall events.

As expected given the riverine environmental context, Zone 1 fluvial polygons (higher flood potential from rivers) within the Core Area are coincident with the Holocene alluvium and the geological deposits of the narrow floodplain surrounding both sides of the River Derwent. Although very limited in spatial distribution, the location of Fluvial Zone 1 polygons within the Buffer Zone highlight areas of interest such as the streams Black Brook and Lumb Brooks situated west of Belper Bridge, the stream

Coppice Brook in Belper, Duffield and the southern part of the DVMWHS Buffer Zone, close to the city of Derby (Figure 5a). The projected increased intensity of winter rainfall events (Met Office, 2009), implies increased susceptibility to flash flooding in the future.

Furthermore Belper Bridge, Ambergate, Whatstandwell and Cromford represent areas with potential for groundwater flooding to occur at surface, meaning that during periods of extended intense rainfall groundwater flooding might occur and manifest at surface inundating above-ground properties. This is investigated in more detail in Section 5.

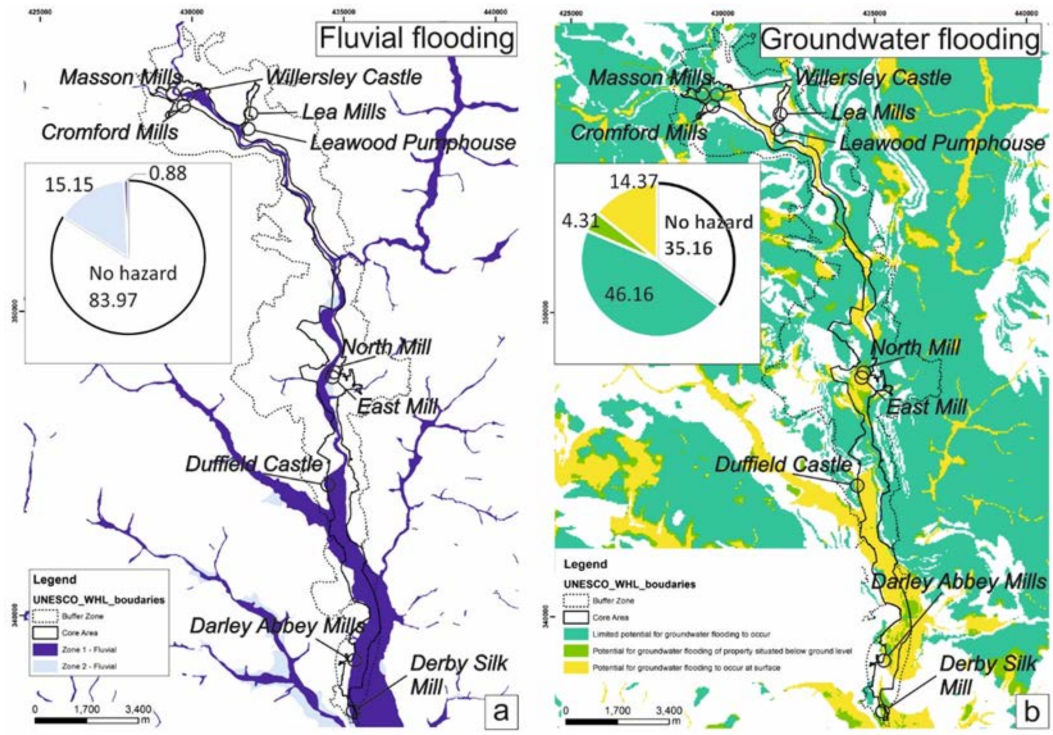

Figure 5. Potential hazards in the DVMWHS associated with fluvial (a) and groundwater flooding susceptibility (b). In (a), Zone 1 corresponds to higher flood potential from rivers: the first areas to experience the effects of inland flooding in a river catchment. Zone 2 corresponds to lower flood potential from rivers: areas affected by secondary flooding in extreme cases as a result of a prolonged flood event. Based upon the Geological Indicators of Flooding dataset, with the permission of the British Geological Survey.

4 Monitoring

4.1 Large scale monitoring

31 Synthetic Aperture Radar (SAR) images acquired during 2015-2017 by the radar satellites Sentinel-1A and Sentinel-1B of the European Space Agency (ESA) have been used to analyse the baseline ground motion scenario of the area of interest (Table 1).

Table 1. List of the 31 input Sentinel-1 scenes that were acquired and processed for the areas of interest. M indicates the master.

id	Satellite	Date	id	Satellite	Date
1	*Sentinel-1A*	*16/11/2015*	*17*	*Sentinel-1B*	*27/01/2017*
2	*Sentinel-1A*	*28/11/2015*	*18*	*Sentinel-1B*	*28/03/2017*
3	*Sentinel-1A*	*10/12/2015*	*19*	*Sentinel-1B*	*09/04/2017*
4	*Sentinel-1A*	*22/12/2015*	*20*	*Sentinel-1B*	*03/05/2017*
5	*Sentinel-1A*	*03/01/2016*	*21*	*Sentinel-1B*	*15/05/2017*
6	*Sentinel-1A*	*15/01/2016*	*22*	*Sentinel-1B*	*27/05/2017 (M)*
7	*Sentinel-1A*	*27/01/2016*	*23*	*Sentinel-1B*	*08/06/2017*
8	*Sentinel-1A*	*20/02/2016*	*24*	*Sentinel-1B*	*20/06/2017*
9	*Sentinel-1A*	*08/04/2016*	*25*	*Sentinel-1B*	*14/07/2017*
10	*Sentinel-1A*	*02/05/2016*	*26*	*Sentinel-1B*	*26/07/2017*
11	*Sentinel-1A*	*26/05/2016*	*27*	*Sentinel-1B*	*07/08/2017*
12	*Sentinel-1B*	*11/10/2016*	*28*	*Sentinel-1B*	*19/08/2017*
13	*Sentinel-1B*	*23/10/2016*	*29*	*Sentinel-1B*	*31/08/2017*
14	*Sentinel-1B*	*04/11/2016*	*30*	*Sentinel-1B*	*12/09/2017*
15	*Sentinel-1B*	*03/01/2017*	*31*	*Sentinel-1B*	*24/09/2017*
16	*Sentinel-1B*	*15/01/2017*			

These satellite scenes, collected through the Interferometric Wide Swath mode in a Single-Look Complex (SLC) format, cover a region of 250 km in range by 180 km in azimuth (Figure 6) and include the key areas of interest of this project, i.e., the industrial landscape along with the modern infrastructures.

The 31 satellite images are characterised by medium ground spatial resolution (~5 m in range and ~20 m in azimuth) and nominal repeat cycle of 6/12 days for each satellite. A data gap in the satellite data exists between May 2016 and October 2016 from when only Sentinel-1B acquisitions were suitable for the DVMWHS. The images were acquired by the SAR sensor operating in C-band (5.3 GHz frequency, 5.6 cm wavelength) when the satellites were flying along their descending orbits (i.e. from north to south) following path 154. The Line of Sight (LOS) employed by the sensor characterised by look angle of 33° with respect to the vertical direction at the centre of the scene, and observe the ground from east to west.

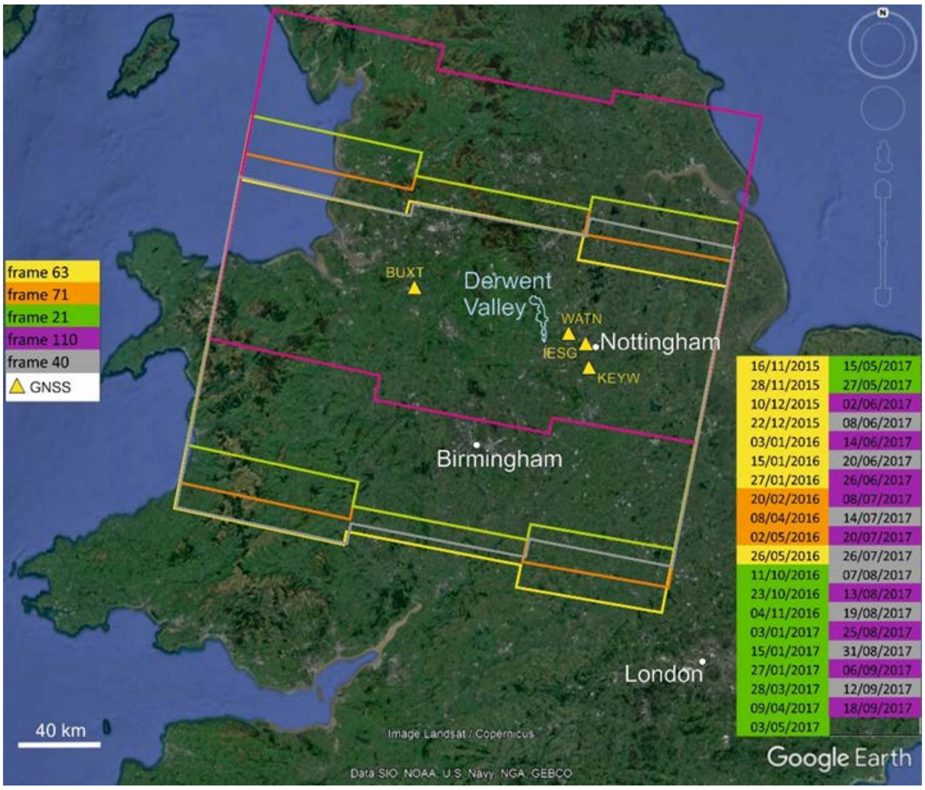

Figure 6. Spatial coverage of the Sentinel-1 2015 to 2017 data with indication of the different areas covered by each frame, Derwent Valley's Buffer Zone and GNSS stations.

Descending geometry has been selected as the main geohazard for natural ground motion, i.e., landsliding on west-facing slopes (Figure 7).

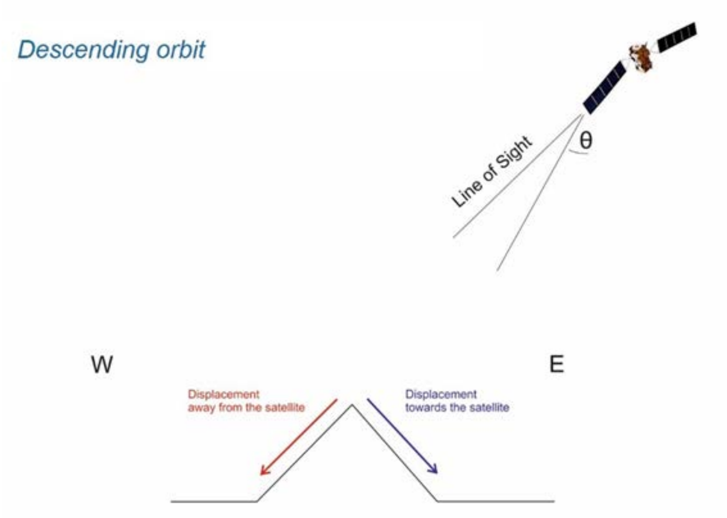

Figure 7. Sketch of geometrical relationship between slope movements and satellite LOS movement.

Multi-temporal image processing of the satellite scenes was undertaken using the GAMMA SAR and Interferometry software, using the Interferometric Point Target Analysis package. This method is based on the generation of a single reference stack to derive the deformation time series from pixels selected by considering temporal variability of SLC intensity which are referred as Permanent Scatterers (PS). This is to minimise the presence of temporal phase decorrelation components in the generated interferograms and enhance phase quality of the processed pixels and preserving their original spacing.

The reference point location to refer all the 2,928,725 ground motion estimates to was set at the IESG GNSS location [338451 N, 454377 E], within an area of high interferometric coherence in the University Park of the Nottingham University where no significant vertical deformation have been observed between 1997 and 2015. In order to validate the reliability of InSAR results, other GNSS deformation rates, available at BUXT, KEYW and WATN, have been compared with the closest PSs (Figure 8).

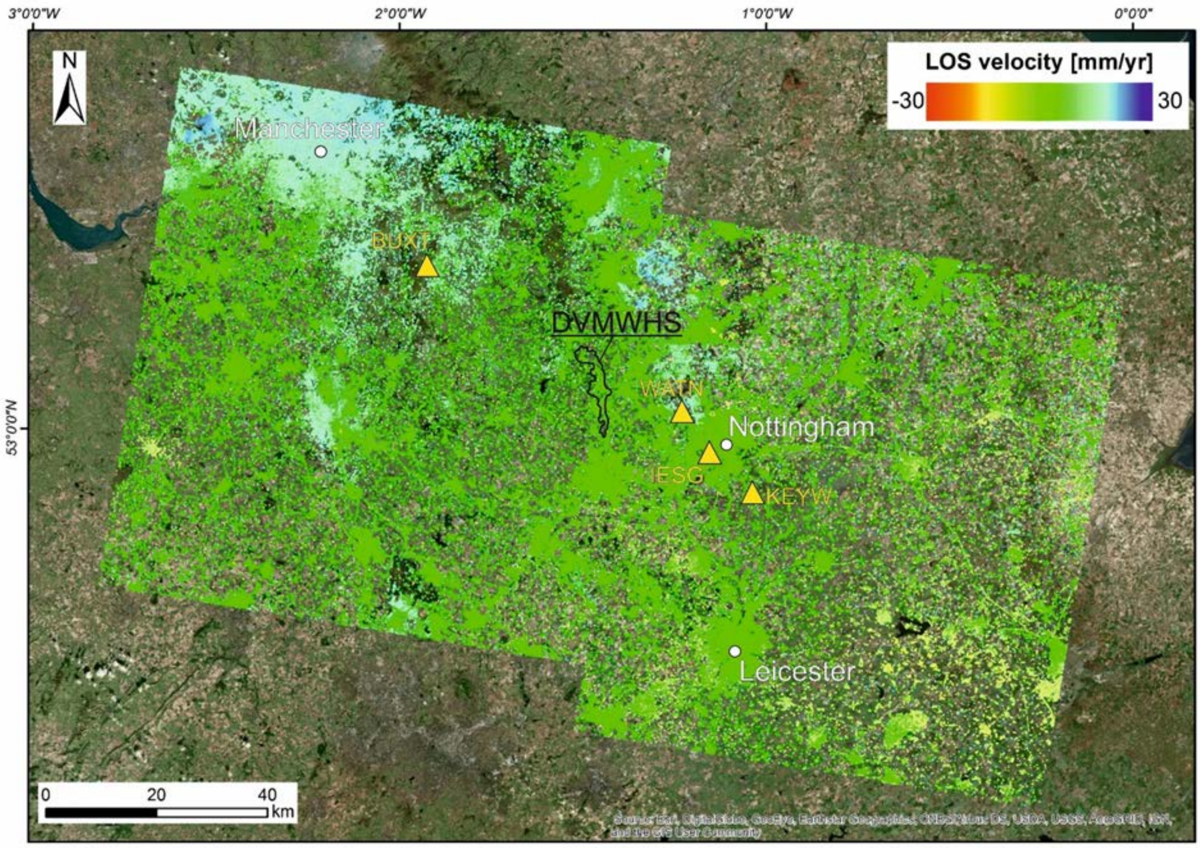

Figure 8. Spatial distribution of the Sentinel-1 InSAR results obtained for an area 7,500 km2 extended.

A total of 12,929 radar targets covers DVMWHS area with a density of 232 PS/km2, an average LOS velocity of 1.04 mm/yr and standard deviation of LOS velocity of 1.23 mm/yr (Figure 9).

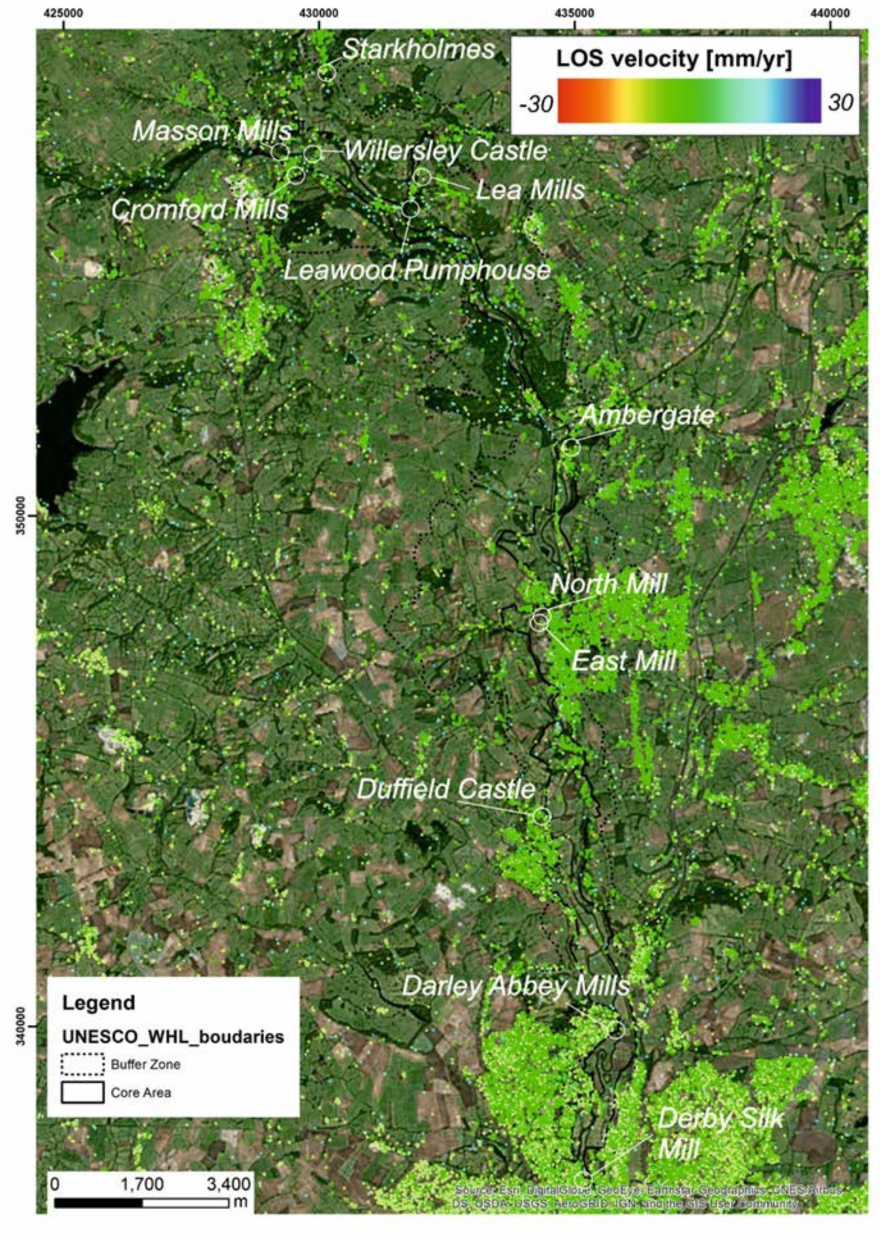

Figure 9. Spatial distribution of the Sentinel-1 results for the DVMWHS area.

According to the average and standard deviation of LOS velocity, a threshold of ±3 mm/yr has been considered to separate moving from non-moving PS: 92% of the DVMWHS PS fall within this category. Despite a significant PS density, their spatial distribution is highly affected by land cover with 54% of the terrain represented by pastures (EEA, 2012).

InSAR results reveal that on average the land is stable, however the three main areas found to be moving have been analysed in detail: Starkholmes landslide (see Figure 4a), Ambergate landslide and Belper North Mill. These are described in section 4.2 below.

4.2 Local scale monitoring

4.2.1 Starkholmes landslide

The Starkholmes landslide [SK301589] lies on the west-facing slopes to the east of Matlock Bath (Figure 10). The village and its contour-following access road lie within the landslide boundary and parts of the landslide have become active within recent years. This activity in the upper slopes has affected several properties in the village and led to subsidence of the Starkholmes Road and Willersley Lane passing through it. The landslide is a complex of multiple deep-seated rotational failures in the upper slope degrading to debris and mudflows immediately below the village on the central and lower slopes. Individual slipped blocks and shallow mudflows tend to follow existing streams. Disruption of surface drainage by construction and dumping has led to elevated pore pressures within the mudrocks of the Bowland High Group (see Figure 2) and contributed significantly to re-activations of historic slides. The northernmost point the slope has been subject to mining activities (Riber lead mine, closed 1959) and a consequent major subsidence event, referred to locally as the 'Big Hole', occurred in October 1992. The trigger for this event was the dumping of spoil on the slope in combination with a very wet summer (Jones, 2008). Mining spoil has also been incorporated into another small-scale landslide re-activation locally and mine waters are known to issue intothe natural slopes beneath.

The 'Starkholmes' landslide stretches southward and joins the 'Woodend House' landslide just north of Cromford Station. Combined, these landslides extend over 2.4 km along the eastern side of the Derwent valley.

In recent years the development of high resolution Digital Terrain Models (DTMs) derived from aerial LiDAR have been able to reveal hidden landslide features as never before; in some instances very subtle features not readily visible on the ground provide further evidence of instability. LiDAR data are complementary to the traditional air photo interpretation (API). These data are available for most of the DVMWHS from the Environment Agency.

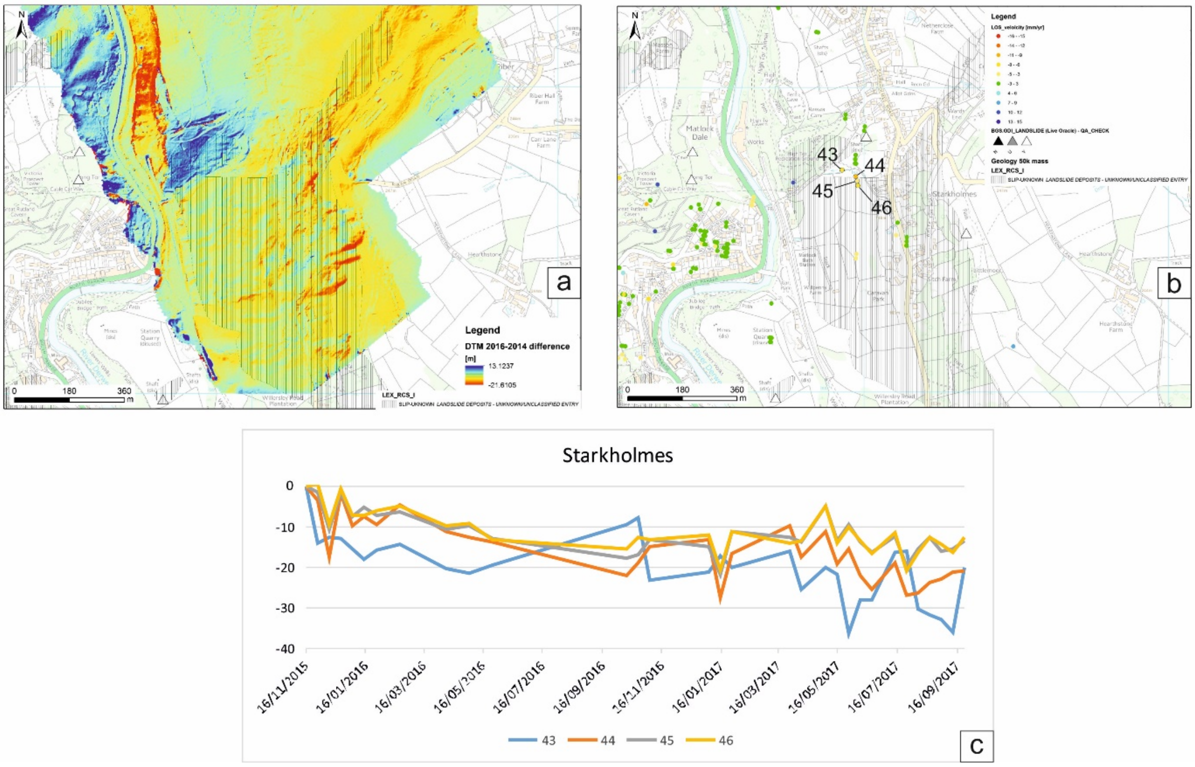

Figure 10. Starkholmes DTMs difference between 2014 and 2016 acquisitions (a), InSAR LOS average velocity (b) and time-series of PS localized in the northern sector of the Starkholmes mass movement (c).

A detail of the InSAR map covering the Starkholmes landslide is shown in Figure 10b. A cluster of negative LOS velocities on the northern flank of the landslide in Starkholmes village indicates a downward movement rate of 3 to 8 mm/yr. The graph shows the progressive movement over a two year period. Most of these points appear to be located on buildings but two in the central part of the landslide are not. The graph for points located in the norther sector indicates an overall movement of 9 mm in two years (Figure 10c).

4.2.2 Ambergate landslide

The second instability analysed in the DVMWHS is Ambergate, situated in the southern half of the area. The landslide is small (0.21 km^2) but in close proximity to a trunk road junction (A6/A610) and the junction of the Derby to Chesterfield and Derby to Matlock railways (Figure 11). It is described in the NLD as a ‘multiple rotational slide and flow’; the depth of which is not known but it is probably deep-seated. The landslide has northerly and north-westerly aspects. The upper slope and western flank are wooded (Thacker’s Wood) and the mid-slope is largely meadow down to the railway while below this the area is given over to small industrial units. The western side of the landslide incorporates the 117 m long Toadmoor Tunnel built in 1840 during the construction of which a landslide occurred necessitating a ‘cut & cover’ engineering solution. The portals of this tunnel are Grade 2 listed structures in the DVMWHS.

The geology consists of Marsden Formation (sandstone and mudstone) and Ashover Grit (sandstone) of the Millstone Grit Group. The mudstones probably contain a significant proportion of shale and as such represent weak, less permeable horizons which were encountered during construction of Toadmoor Tunnel, remediation of subsequent tunnel deformation due to renewed landslide movement having been required. The Geosure landslide rating is mainly the highest value of E with some C and D.

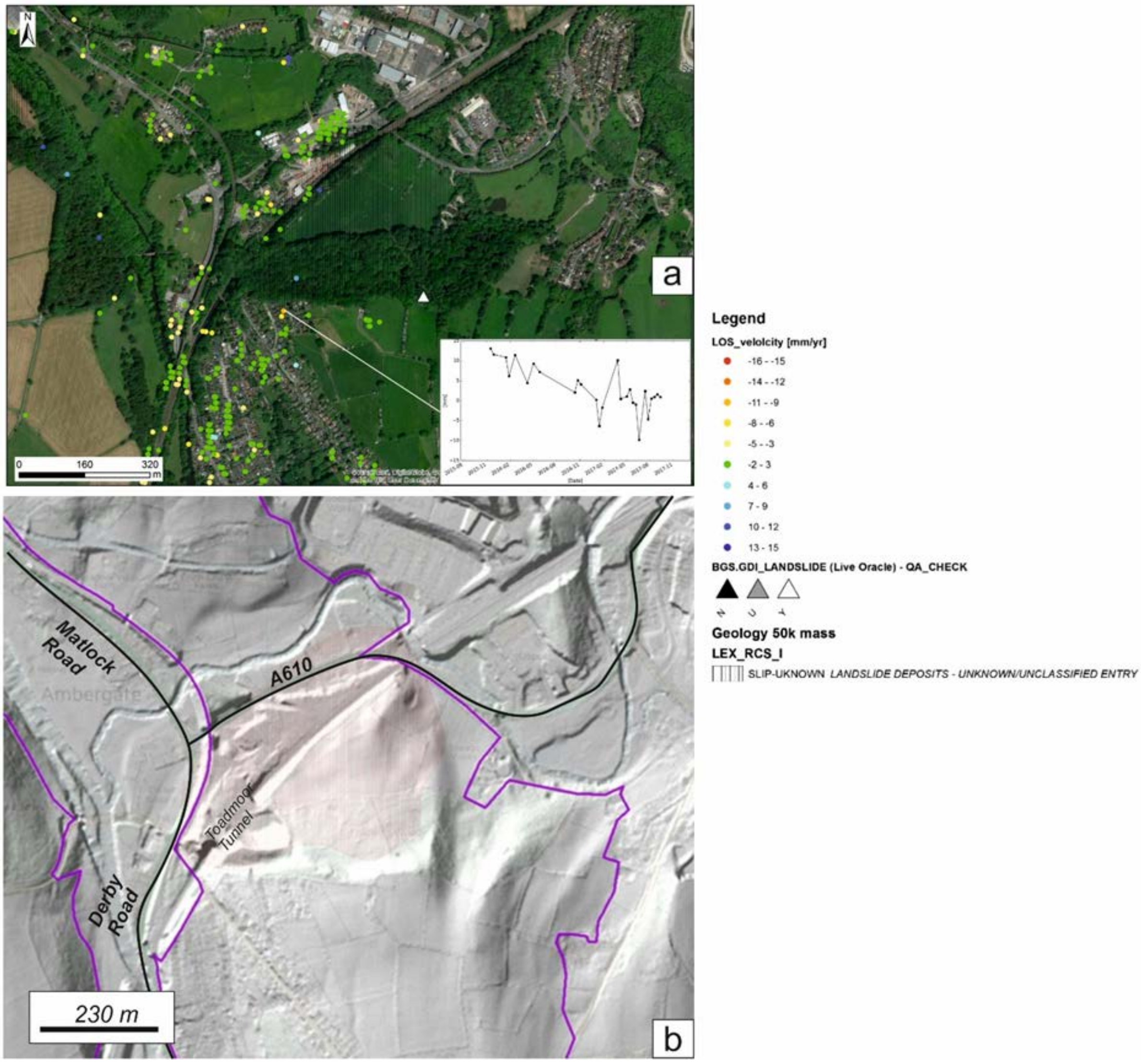

Figure 11. Ambergate, InSAR LOS average velocity (a) and LiDAR 2m DTM of 2016 (b). Contains Environment Agency information © Environment Agency and database right 2016.

The InSAR data for Ambergate (Figure 11a) show four points that are considered significant downward movements (rates of 6 to 11 mm/yr) within the NLD landslide polygon, involving the line of Toadmoor Tunnel and the industrial area at the foot of the slope adjacent to the A610, which may indicate ongoing movement of the tunnel and its surroundings.

The LiDAR DTM (Figure 11b) shows a disturbed zone in the vicinity of Toadmoor Tunnel, presumably dating to tunnel construction but with little to suggest a landslide in the remaining parts of the NLD landslide polygon, apart from the backscarp and possible displacement of the course of the River Amber at the toe; though the latter is uncertain.

4.2.3 Ground movement near historic mills

While Starkholmes and Ambergate instabilities do not directly affect any of the historic cotton and silk mill complexes, in Belper InSAR results show movements within the Core Area, threatening both the North Mill and East Mill (Figure 12).

Figure 12. Belper, InSAR LOS average velocity (a).

For the Belper area the main geohazards susceptibility is connected to fluvial and groundwater flooding. Therefore, the subsidence observed on the south-east corner of the East Mill (Figure 12) can be related to building foundation damage following the 2007 flooding, still visible in the basement of the North Mill (Figure 13). The uplift east of the North Mill instead can be related to anthropogenic activities given the strong correlation in space and time of the displacement patterns following the

Winter 2016-17 flooding of the area whose damage are still visible in basements and foundations of the North Mill (Figure 13).

***Figure 13**.Visit to The North Mill, Belper, by the PROTHEGO team (October 2017). Left: evidence of the recent flooding events shown in the supportive pillars in the basement. Top right: Adrian Farmer (Derwent Valley Mills Heritage Co-ordinator) in the North Mill basement, explaining the recent flooding issues. Bottom right) External view of The East Mill.*

5 Modelling for a changing climate

Changes in climate will undoubtedly alter the susceptibility of the WHS to geohazards. Changes in the rainfall and snowfall regimes will impact on drainage patterns, landslides and flooding occurrence and the annual soil moisture deficit patterns. UKCP09 (The United Kingdom Climate Projections 2009) provide future climate projections for the UK, from the 2020s to 2080s. They are the product of the Met Office’s Hadley Centre and over 30 other contributing organisations. They are based on sound research and are considered the most comprehensive source of climate information for the country. Originally unveiling 3 emissions scenarios (high, medium and low), there has been evidence in recent times that the medium to higher emissions scenarios are most likely (Friedlingstein et al., 2014).

For the Derwent catchment, at both medium and high emissions scenarios, the area is projected to experience drier, warmer summers, wetter winters with higher intensity rainfall events, with similar overall annual rainfall (Figure 14 and Table 2). This could lead to events such as that in January 2013, when the River Derwent swelled, causing flooding, due to heavy rain and melting snow, becoming more frequent in the future (Figure 15) and impact on geohazard occurrence in the WHS.

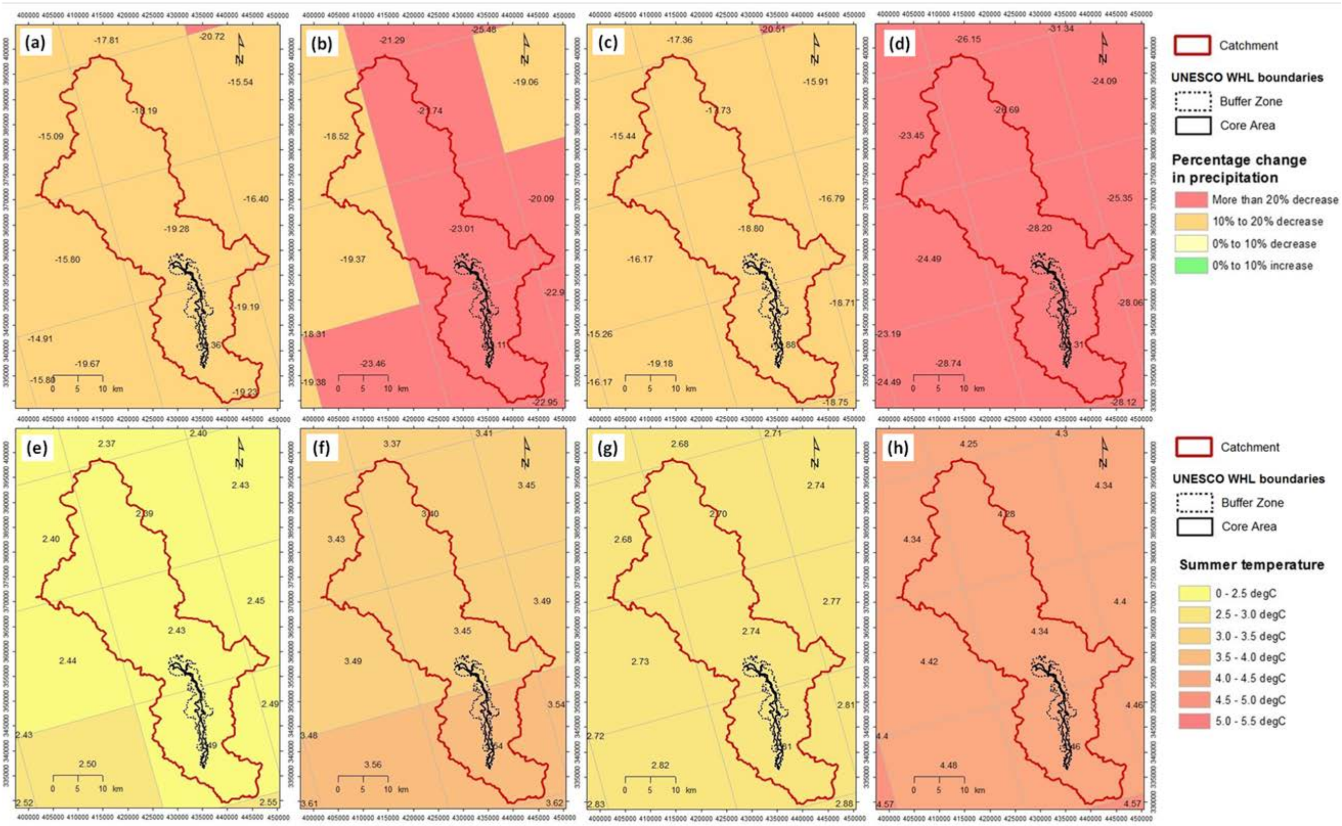

Figure 14: UKCP09 projections for summer (a-d) precipitation and (e-h) temperature for the scenarios: (a,e) 2050s, medium emissions; (b,f) 2080s, medium emissions; (c,g) 2050s, high emissions; and (d,h) 2080s, high emissions for the the Derwent river catchment area at the confluence with the Trent river [Derwent catchment boundary: CEH © NERC. All rights reserved; UKCP09 © Crown Copyright 2009].

UKCP09 projections	Central estimate 2050 medium emissions		Central estimate 2050 high emissions		Central estimate 2080 medium emissions		Central estimate 2080 high emissions	
	Min change	*Max change*	*Min change*	*Max change*	*Min change*	*Max change*	*Min change*	*Max change*
Summer precipitation (% change)	-15.1	-19.4	-15.4	-18.9	-18.5	-23.1	-23.4	-29.3
Summer mean temperature (°C)	2.4	2.5	2.7	2.8	3.4	3.5	4.2	4.5
Annual mean precipitation (% change)	0.1	-0.1	-1.5	-2.0	-0.2	0.5	0.3	0.6

Table 2: UKCP09 medium and high emissions projections for the Derwent river catchment area.

Figure 15: Left) January 2013, The Big Thaw caused increased flow in the River Derwent, Belper (© Page One). Right) Lower river flow in the River Derwent, Belper, during PROTHEGO project visit in October 2017.

5.1 Landslides and a changing climate

Shallow translational and rotational landslides are strongly controlled by antecedent effective rainfall, with significant increases in susceptibility following a high intensity rainfall event (Pennington et al., 2014). UKCP09 projects winter high intensity rainfall events will increase in magnitude by approximately 10% under both medium and high emissions scenarios (Met Office, 2009), leading to increased susceptibility to associated landslide-prone areas (Cigna et al., 2016).

5.1.1 'SLIM' flooding model

The 'SLiM' flooding model provides various predictive parameters nationally on a 200 m cell size. Parameters include Rainfall, Soil Moisture Deficit (SMD), Actual Evapotranspiration (AET) and Near Surface Shallow Storage (NSSS). These represent parameters are applicable to landslide re-activation.

The environmental parameters covering a particular landslide event (Starkholmes, 26th June, 2012) are shown graphically in Figure 16. The Rainfall is shown in a blue box, the soil moisture deficit (SMD) in two red boxes, Near Surface Soil Storage (NSSS) plot in an orange box and the Actual Evapotranspiration (AET) in a purple box. In each case the landslide event is marked by a red circle. It is notable that the landslide event coincides with an unusually low SMD (at least compared with 2011 and 2013) which occurred in June 2012 within a wider and notably irregular summer pattern which is also reflected in a period of high summer rainfall. InSAR results confirm that the movement is still ongoing at a constant rate (see section 4.2).

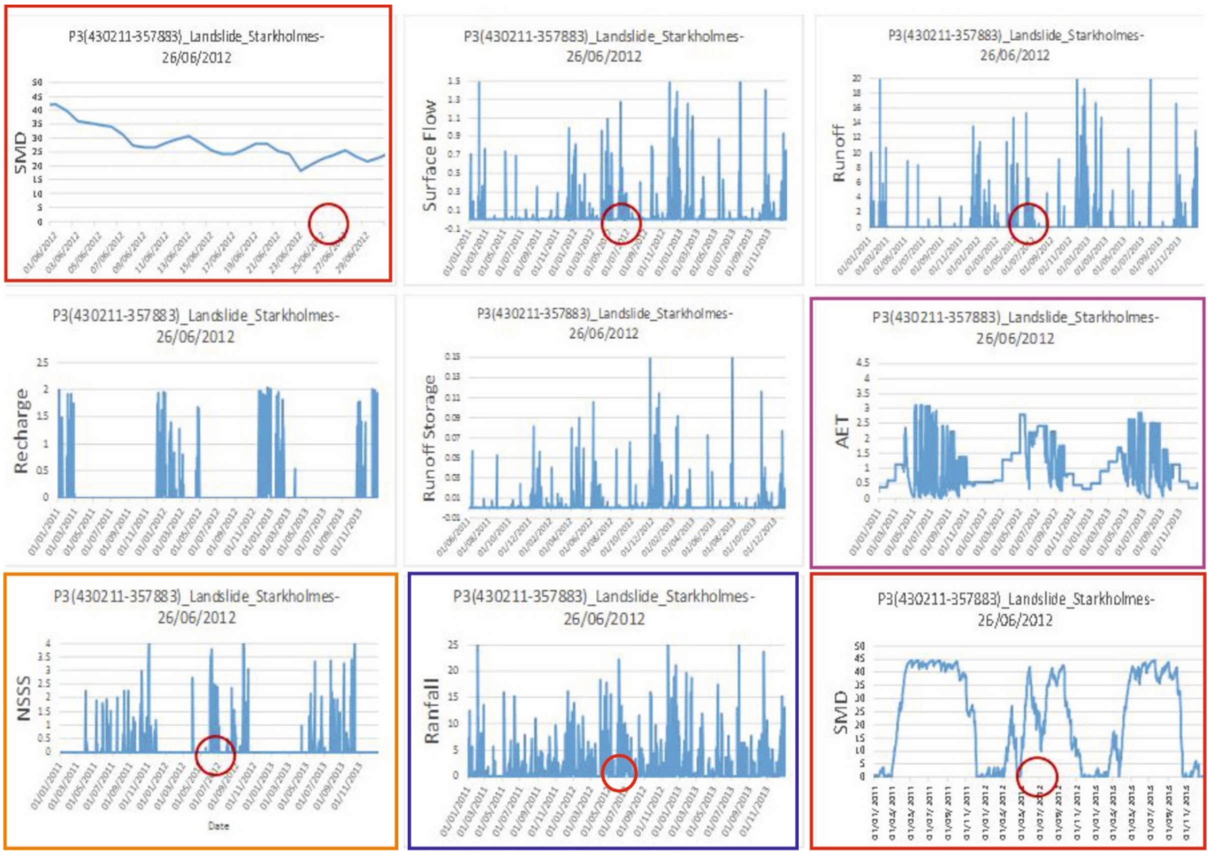

Figure 16: Variation of environmental parameters for June 2012 and Starkholmes landslide event (26/06/2012) shown as red circle

Other examples of landslide events in the DVMWHS also appear to coincide with low Soil Moisture Deficit (SMD) values, when soils are wetter; for example, the Belper event of 25th December 2012 (Figure 17). The SMD may be a better indicator of landslide events than rainfall, though time series are currently too short and landslide events too few to be conclusive on this point.

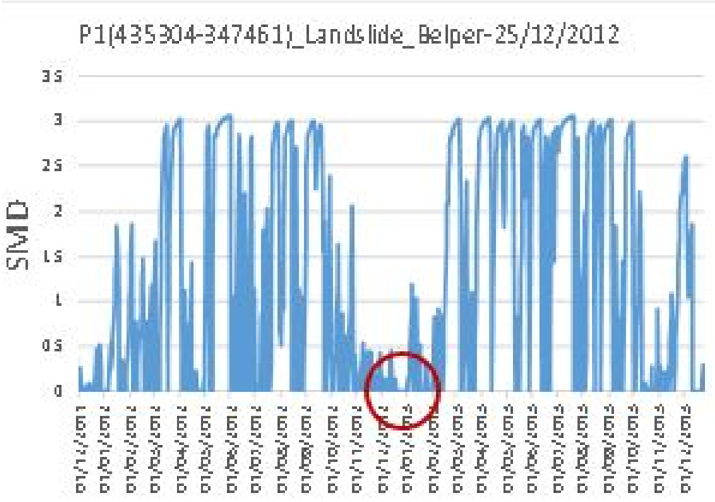

Figure 17: Soil Moisture Deficit (SMD), Dec 2011 to Dec 2013, for Belper landslide event (25/12/2012)

5.1.2 Landslide: hazard and risk

Possible hazards and risks to the DVMWHS emanating from landslide activity may be summarised as follows:

1. Direct impact on buildings and infrastructure.
2. Blocking of river courses resulting in widespread flooding.

Initiation of 'new' landslide in previously unslipped ground and / or re-activation of landslides may result from the following:

- Intense localised rainfall events.
- Increased rainfall averages and intensities due to climate change.
- Landslide toe de-stabilisation due to river bank erosion.
- Changes of land use (e.g. de-forestation)
- Disrupted drainage
- Engineering activity (e.g. road construction)
- Flooding

Consideration of the elements of the DVMWHS at risk from landslides, whilst concentrating on the mill buildings themselves, should also include a wide range of other contemporaneous structures and infrastructure, for example workshops, pumping stations, railways, inclined planes, canals, milllsetc. As most of these elements are situated in the valley floor they may be at risk from landslides on the valley slopes, either directly or indirectly; for example, by direct impact or by flooding due to damming of rivers caused by landslide or by river bank erosion. Also in the DVMWHS there is the addition of former mines, shafts and adits to the risk of ground collapse at surface, formation of sinkholes and initiation of landslides. These are summarised in Figure 18.

Consideration should also be given to modern infrastructure such as road, rail and utilities (gas, electricity, water supply/drainage) as these provide transport, energy, sanitation etc. for residents, employees and visitors in the DVMWHS; the disruption of which may also constitute multifarious hazards (e.g. gas leak, sinkhole, water contamination).

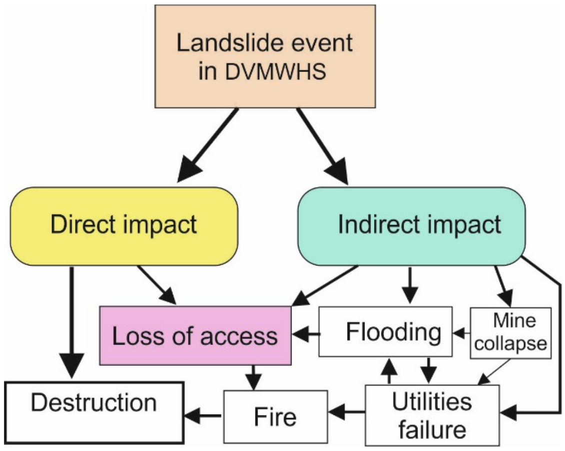

Figure 18 Schematic showing possible impacts of landslide event in the DVMWHS

Susceptibility to landslides is covered by the BGS's Geosure model which has national coverage. This classes slopes from A to E where A is stable and E unstable and where recorded landslides are included as E. Within the DVMWHS the Geosure classes D & E are widespread and include around 16 recorded landslides of different sizes and states of activity or inactivity. In parts of the Derwent Valley slopes are continuously classed D & E over several kilometres and recorded landslides have a tendency to coalesce. It has been demonstrated, by example, that many of these landslides are complex and deep-seated and in some cases (parts of) these landslides have become active on a historic time scale. It is also the case that small rockfalls and mudflows are likely to remain un-recorded and may also lie outside Geosure classes D & E. Geosure statistics for the DVMWHS are shown in Table 3. This table shows that Geosure classes D & E occupy 14.7% (combined) of the total (buffered) area with class B dominant at 62%.

Table 3: Table of Geosure Landslide classes for DVMWHS

Class	Area (km^2)	Area %
A	0	0
B	34.5	61.9
C	13.1	23.4
D	4.8	8.6
E	3.4	6.1

5.2 Subsidence

Subsidence due to shrink-swell clays is ground movement caused by the swelling and shrinking of clay-rich soils, due to soil moisture fluctuations causing volume change. Therefore, in susceptible areas, subsidence is largely driven by antecedent rainfall and temperatures, with hazard susceptibility projected to alter due to changes in rainfall patterns. The projected change in the amount and distribution of rainfall to the UK (Met Office, 2009), as a result of climate change, could suggest a significant increase in the damage done in the country by the shrinking and swelling behaviour of these clay soils.

BGS have been developing a new "GeoClimate – clay shrink swell" product, which combines climate change projections, current GB subsidence hazard susceptibility and a GB groundwater model to project future subsidence GB hazard. The datasets utilised and combined in GeoClimate (Harrison et al., 2017) are:

- **11 RCM UKCP09 climate models**: UKCP09 medium emissions scenario was used to force the 11 Regional Climate Model simulations, providing absolute values to input into GeoClimate. The values provided are continuous daily projections from 1950 to 2099 (Murphy *et. al.*, 2009).
- **BGS GeoSure Subsidence**: BGS GB dataset providing geological information on potential subsidence, providing 5 classes from Hazard Rating A (pre-dominantly non-plastic ground conditions) to Hazard Rating E (predominantly very high plasticity ground conditions) (Walsby, 2008)

- **Zooming Object Oriented Distributed Recharge (ZOODRM) model**: Provides gridded daily soil moisture deficit (SMD) values for UK, based on inputted rainfall and surface values (Mansour & Hughes, 2014).

Running the GeoClimate model, based on the medium greenhouse gas emissions scenario, and viewing the average, driest and wettest projections for the DVMWHS revealed low projected clay shrink-swell susceptibility, in the core zone and buffer zone. Figure 19 shows the 2080 driest projection, as a demonstration of the "worst case scenario" for the site. This indicates that by 2080, it is projected that building foundations could possibly be affected by clay shrink-swell in a relatively small area in the south of the Derbyshire Derwent catchment.

Based on UKCP09 climate projections until the 2080s, it is unlikely that subsidence due to clay shrink-swell will become a significant hazard in the Derwent Valley Mills WHS, due to changes in climate.

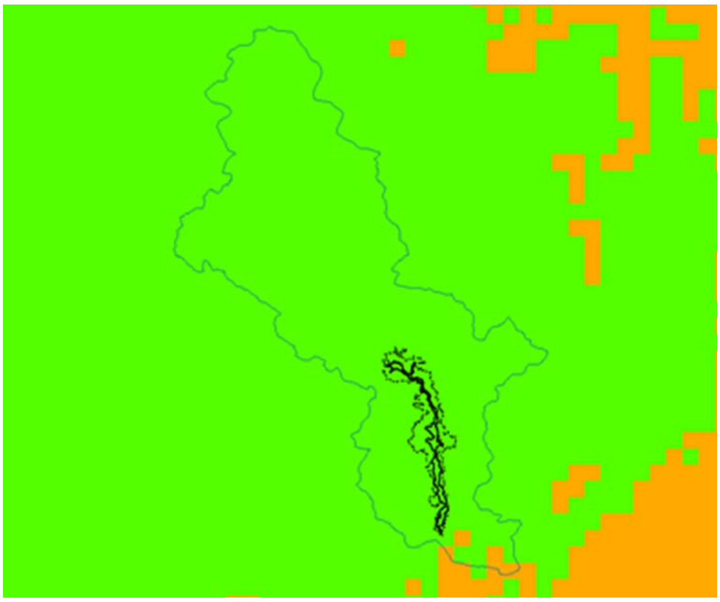

Colour	Associated susceptibility text
Green	It is 'doubtful' that foundations will be affected by shrink/swell occurrence under these climatic conditions.
Orange	It is 'possible' that foundations will be affected by shrink/swell occurrence under these climatic conditions.
Red	It is 'probable' that foundations will be affected by shrink/swell occurrence under these climatic conditions.

Figure 19: The DVMWHS core area and buffer zone, with the Derbyshire Derwent Catchment. The GeoClimate projection for subsidence susceptibility in 2080 (driest)

5.3 Flooding

Groundwater Flooding is controlled by antecedent soil moisture capacities, rainfall intensities and durations. The projected increased intensity of winter rainfall events (Met Office, 2009), implies increased susceptibility to flash flooding in the future. The location of the mills and heritage infrastructure within the landscape, proximal to the River Derwent, make them particularly susceptible to flooding as a result of high flow rates associated with high intensity rainfall events (Cigna et al., 2016).

5.3.1 Modelled results and climate change scenario runs

The Soil and Landuse based rainfall-runoff and recharge Model (SLiM) links runoff and recharge processes to rainfall intensity, potential evapotranspiration, and catchment characteristics, such as soil type, land cover, topography, and baseflow index (Wang et al., 2012). It introduces the concept of soil moisture deficit (SMD), excess water and bypass runoff and calculates both recharge and runoff. For this project, it has been successfully adopted at the DVMWHS to estimate future recharge at the catchment scale (See Appendix 1 For details of the methodology applied).

To assess the effect of a changing climate on flooding hazard susceptibility in Derwent Valley Mills WHS, the climate data for 11 Regional Climate Models (as introduced in Section 5.2) were entered into the calibrated catchment-scale and national-scale models to predict future hydrological processes under the climate change models. The historical and future daily distributed datasets were produced: soil moisture deficit, surface flow, runoff, recharge, runoff storage, actual Evapotranspiration, near surface shallow storage.

For example, Figure 20 shows the estimated groundwater recharge for Great Britain in the dry and wet seasons. The historical results were used to analysis and calibrate the landslide and flooding events.

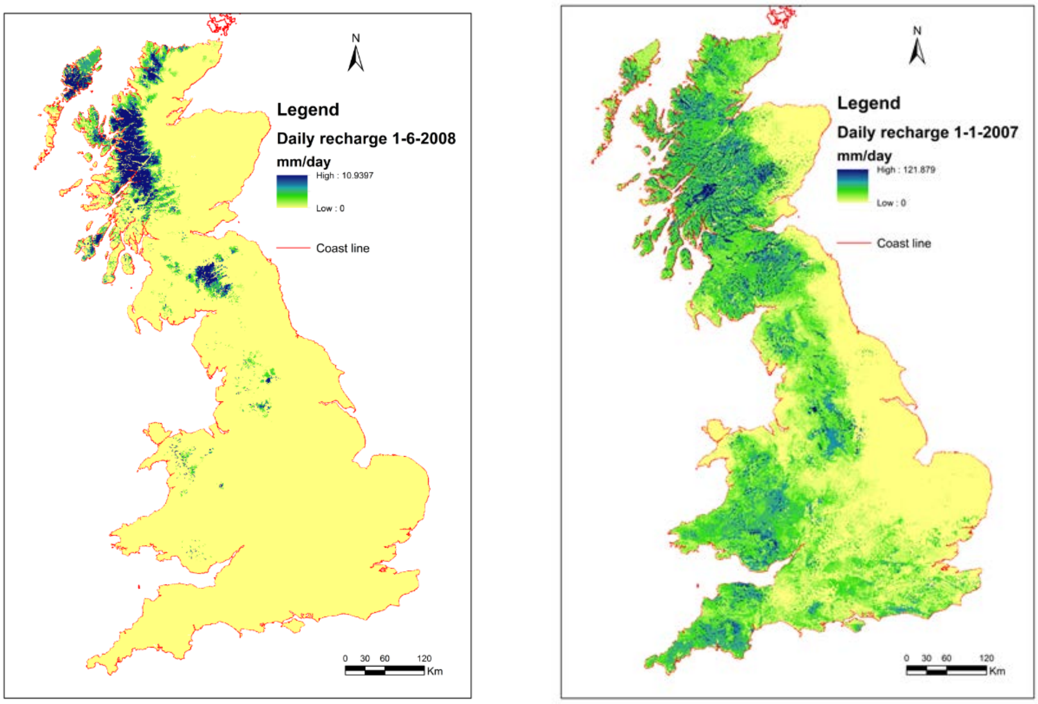

a) b)

Figure 20: Estimated recharge for Great Britain in the dry season (a) and wet season (b)

5.3.2 Flooding susceptibility index

Based on the analysis of linkage of hydrological components to historical events, an index method was developed to calculate the flooding susceptibility ($FloodSus$):

$$FloodSus = W_{sf}I_{sf} + W_{ro}I_{ro} + W_{sfs}I_{sfs} + W_{rech}I_{rech} + W_{SMD}I_{SMD} \quad (8)$$

$$I_{sf} = \frac{SurfaceFlow}{Max_{SurfaceFlow}}; \quad (9)$$

$$I_{ro} = \frac{Runoff}{Max_{Runoff}}; \quad (10)$$

$$I_{sfs} = \frac{SurfaceFlowStorage}{Max_{SurfaceFlowStorage}}; \quad (11)$$

$$I_{rech} = \frac{Recharge}{Max_{Recharge}}; \quad (12)$$

$$I_{SMD} = 1 - \frac{SMD}{Max_{SMD}}; \quad (13)$$

where I_{sf}, I_{ro}, I_{sfs} , I_{rech} , and I_{SMD} are indices of surface flow, runoff, surface flow storage, groundwater recharge and soil moisture deficit; and W_{sf}, W_{ro}, W_{sfs} , W_{rech} , and W_{SMD} are the weighting values of these factors and can be identified using the historical flooding events (Figure 21).

Based on the calibrated index method, the flooding susceptibility maps for the future have been generated. Figures 22 and 23 show the flooding susceptibility of the Derwent catchment and Great Britain on 1/7/2050 and 1/1/2080 using the *afixi* RCM scenario.

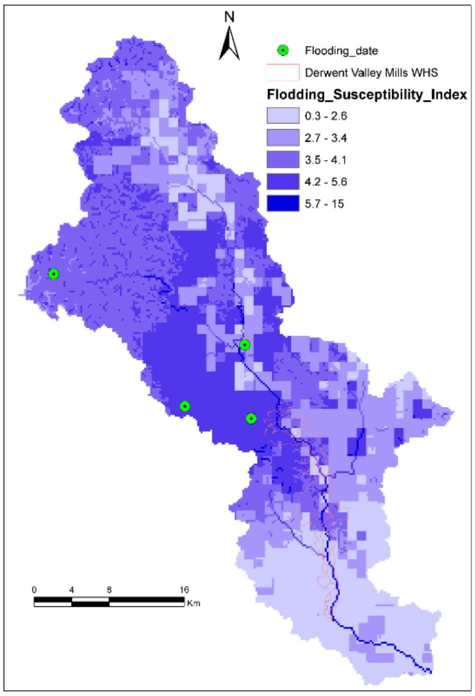

Figure 21: Calibrating the flooding susceptibility index method using the historical flooding event at Derbyshire on 10/8/2004

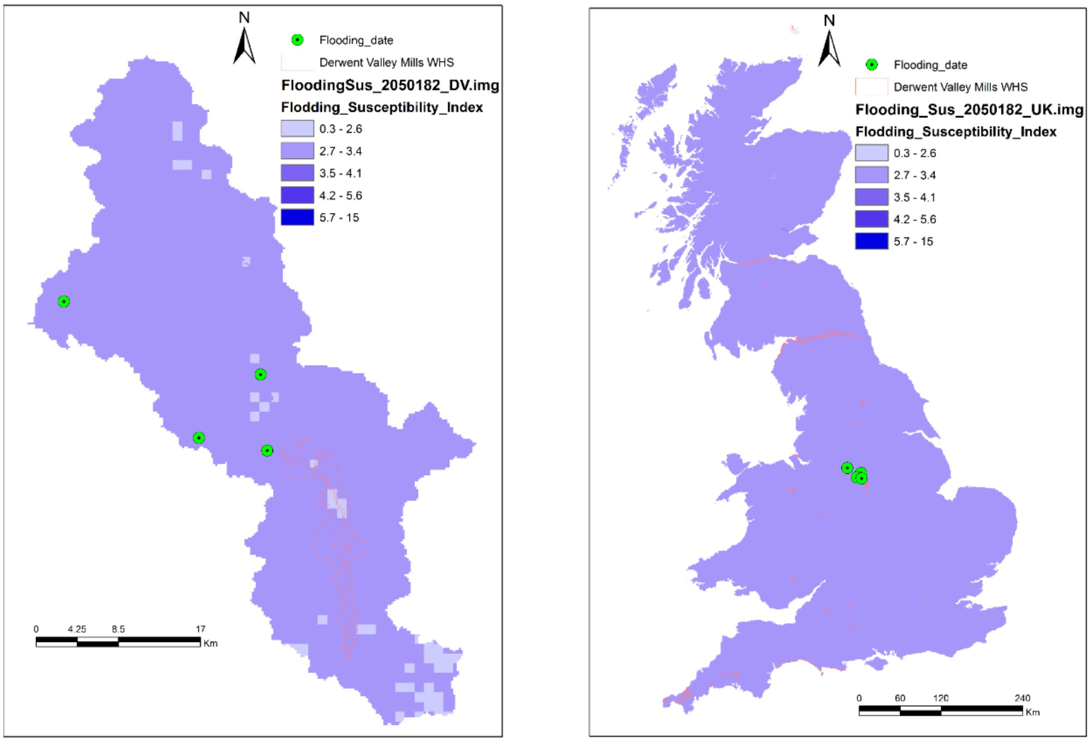

Figure 22: Flooding susceptibility of the Derwent catchment and Great Britain on 1/7/2050 using the afixi RCM scenario

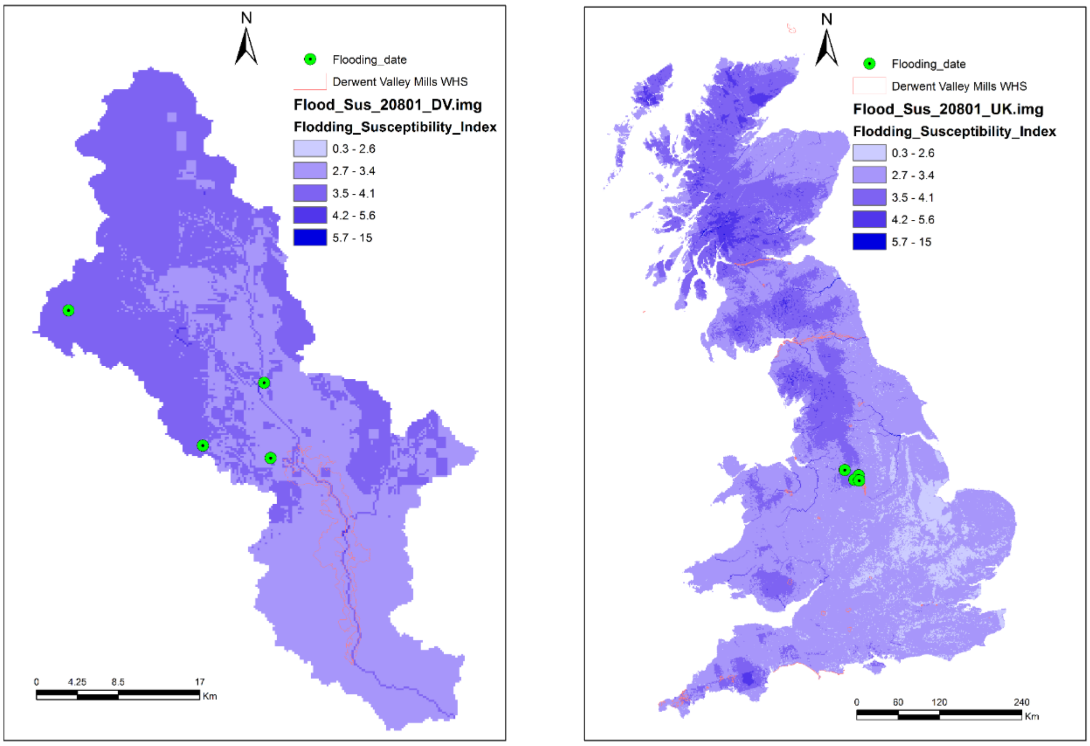

Figure 23: Flooding susceptibility of the Derwent catchment and Great Britain on 1/1/2080 using the afixi RCM scenario

6 Discussion

Overall, BGS GeoSure geohazard datasets demonstrate that the majority of the DVMWHS combined core and buffer zone area is attributed to very-low to low susceptibility for collapsible and compressible ground, clay shrink-swell, debris flow, running sand and soluble rock hazards. Landslide susceptibility for the area is slightly higher, with landslides distribution and current activity not directly impacting the World Heritage constructions.

Furthermore, the study has examined the potential effects of changing geohazard patterns for landslides, subsidence and flooding under the current climate projections given the size, state of activity and distribution of these three hazards.

However, any attempt to integrate monitoring and modelling data was not possible, the main problems being the joining together of disparate datasets, such as those described above (LiDAR, NLD and InSAR) with equally disparate susceptibility models (Geosure and SLIM), the different time and geographical scales. Each provides important information about landslide activity but providing a causal link is not easy where time scales of a few months or years are concerned. This is because landslide events, whether fresh or re-activated, in Britain generally, and the DVMWHS specifically, are unusual and more often than not go unnoticed. Most recorded landslide activity is in the form of partial re-activation of pre-existing landslides dating from the end of the last Ice Age. Target coverage and errors in target geolocation (~10 m) affecting the InSAR results have been the main constraints in this work. The first limited the analysis of ground motion data to man-made objects while the latter prevented the systematic use of the data for single infrastructure structural assessment.

However, the results obtained so far prove the benefit of InSAR for the monitoring activity in the DVMWHS in achieving an updated knowledge of the existing criticalities, as well as of the situations of potential instability at a slope-scale.

Any ability to correlate landslide movements with the environmental data available from SLIM must be tempered by the fact that these are ‘modelled’ rather than actual results. However, taken on a catchment-sized scale and over a prolonged time period these models can be useful. One way in which connections can be made is to set up ‘thresholds’ for example of rainfall or SMD beyond which some form of landslide re-activation may be anticipated or even predicted. This requires longevity of datasets and/or intensive landslide activity to have any hope of success in the British environment.

7 Conclusions

The Derwent Valley Mills World Heritage Site is inherently vulnerable to certain geohazards due to the geographical setting of the site and the close location of the heritage buildings to the water course.

This study reveals that the principal geohazards of concern within the DVMWHS are landslides and fluvial and groundwater flooding. The other shallow geohazards assessed within the study area (clay shrink-swell, compressible ground, collapsible deposits, running sand and soluble rocks) have a comparably lower susceptibility, and the consequences would potentially be smaller. These considerations confirm the preliminary geohazard assessment conducted in Cigna et al. (2016).

In particular, two landslide locations are identified that could impact the World Heritage Site in the future: these are the Starkholmes and Ambergate sites where InSAR data confirms the landslide susceptibility data concerning the active state of the high susceptibility landslide hazard. In Belper, the radar data identified the damage connected to the recent flooding event.

The findings of this study can inform planning and mitigation activities by site managers, enabling users to confidently identify areas with increased geohazard susceptibility and build an understanding of the potential consequences to key heritage locations.

The methodology introduced in this report, preliminary employing a geological review including analysis of national scale geohazard susceptibility datasets to identify variations in hazard susceptibility, then utilising remotely sensed data (e.g. InSAR) to carry out a detailed local scale assessment of the current natural hazards, has be shown to be valuable and could be extended to other World Heritage Sites. Additionally, a modelling of the future landslide, subsidence and flooding susceptibility has been evaluated according to the UK climate projection from the 2020s to 2080s.

The application of the methodology to not only the core zone, but also the buffer zone, and in some cases the wider catchment, is crucial in understanding potential geohazard impacts on a World Heritage Site.

This work has highlighted the potential for future research to aid the protection of WHSs from the two main potential sources of hazard within the site: landsliding and flooding, but, there has been no suggestion on implementing specific mitigation measures or on the cost-benefit analysis of possible mitigation alternatives lacking a comprehensive analysis of disaster vulnerability, risk and resilience. However, modified drainage patterns, dependant on localised conditions (wells and drains), drainage maintenance, floodwalls and floodgates, raising community awareness (flood risk maps) to allow individuals to take action appears to be the initial response to these shallow processes. Additionally, antecedent rainfall is a major driver of the occurrence of both, and therefore the frequency and magnitude of these geohazards will be affected by future climate change. With the release of UKCP18 projections imminent, this is also an opportunity to strengthen the resilience of UNESCO heritage sites to future climatic fluctuations.

7.1 Abbreviations

AET	Actual Evapotranspiration
API	Aerial Photo Interpretation
BGS	British Geological Survey
DTM	Digital Terrain Model
DVMWHS	Derwent Valley Mills World Heritage Site
EA	Environment Agency
InSAR	Interferometry Synthetic Aperture Radar
LiDAR	Light Detection And Ranging
NLD	National Landslide Database (BGS)
NSSS	Near-Surface Shallow Storage
SLiM	Soil and Land-use based rainfall-runoff-recharge Model
UKCP09	UK Climate Projections 2009

References

BRITISH GEOLOGICAL SURVEY, 2016. BGS Data Products. Susceptibility to groundwater flooding. Explanatory notes for users, 4 pp.

BRITISH GEOLOGICAL SURVEY, 2014. Compressible Ground. UK Geohazard Note, June 2014. 3 pp.

BOOTH, K. A., DIAZ DOCE, D., HARRISON, M., & WILDMAN, G. (2010). User guide for the British Geological Survey GeoSure dataset. British Geological Survey Internal Report, OR/10/066. 17pp.

BOOTH, K. AND WILDMAN, G., 2010. Geological Indicators of Flooding: User Guidance Notes, 2010. BGS Open Report OR/10/064, Nottingham, UK, 10 pp.

CHENEY, C.S. (2007) The hydrogeology of the Chesterfield, Matlock and Mansfield district (Geological Map Sheet 112), British Geological Survey.

CIGNA, F., HARRISON, A., TAPETE, D., LEE, K., 2016. Understanding geohazards in the UNESCO WHL site of the Derwent Valley Mills (UK) using geological and remote sensing data. In Fourth International Conference on Remote Sensing and Geoinformation of the Environment (pp. 96881V-96881V). International Society for Optics and Photonics.

COOPER A.H., FARRANT A.R., PRICE S.J. 2011. The use of karst geomorphology for planning, hazard avoidance and development in Great Britain. Geomorphology, 134 (1-2), 118-131.

EUROPEAN ENVIRONMENT AGENCY, EEA, 2012. Implementation and Achievements of CLC2006 65 pp.

FARRANT, A.R. AND COOPER, A.H., 2008. Karst geohazards in the UK: the use of digital data for hazard management. Quarterly Journal of Engineering Geology and Hydrogeology, 41 (3), 339-356.

FOSTER, C., PENNINGTON, C. V. L., CULSHAW, M. G., LAWRIE, K., 2012. The national landslide database of Great Britain: development, evolution and applications. Environmental earth sciences, 66(3), 941-953.

GIBSON A.D., CULSHAW M.G., DASHWOOD C., PENNINGTON C.V.L. 2013. Landslide management in the UK—the problem of managing hazards in a 'low-risk' environment. Landslides, 10 (5), 599-610.

HARRISON A.M., D ENTWISLE, L JONES, M LARK, M MANSOUR, J RICHARDSON, L WANG, J WHITE, A HULBERT, K LEE., 2017. Climatic Hazards and Natural Geological Events (CHANGE): Project report 2015-2016 Development Report. BGS Internal Report IR/15/010.

HOWARD, A. J., KNIGHT, D., COULTHARD, T., HUDSON-EDWARDS, K. A., KOSSOFF, D., MALONE, S., 2015. Assessing riverine threats to heritage assets posed by future climate change through a geomorphological approach and predictive modelling in the Derwent Valley Mills WHS, UK. Journal of Cultural Heritage, 19, 387-394.

JONES, J., 2008. The big hole of Starkholmes. Mercian Geologist, Vol. 17 (1), pp19-22.

MANSOUR, M.M.; HUGHES, A.G. 2014. Land use, climate change and water availability: preliminary modelling of impacts of climate change and land use change on groundwater recharge for England and Wales. Nottingham, UK, British Geological Survey, 53pp. (OR/14/018) (Unpublished) http://nora.nerc.ac.uk/507537/

MET OFFICE, 2009. UKCP09 Climate Projections, 2009. (Accessed on 20 July 2017, http://ukclimateprojections.metoffice.gov.uk)

MURPHY, J.M., SEXTON, D.M.H., JENKINS, G.J., BOORMAN, P.M., BOOTH, B.B.B., BROWN, C.C., CLARK, R.T., COLLINS, M., HARRIS, G.R., KENDON, E.J., BETTS, R.A., BROWN, S.J., HOWARD, T. P., HUMPHREY, K. A., McCarthy, M. P., McDonald, R. E., Stephens, A., Wallace, C., Warren, R., Wilby, R., Wood, R. A. (2009), UK Climate Projections Science Report: Climate change projections. Met Office Hadley Centre, Exeter. http://ukclimateprojections.defra.gov.uk

Pennington, C. V. L., Dijkstra, T. A., Lark, M., Dashwood, C., Harrison, A. M., Freeborough, K. A. and Reeves, H. J. "Antecedent precipitation as a potential proxy for landslide incidence in the UK," Proc. Third World Landslide Forum, Landslide Science for a Safer Geoenvironment 253-259 (2014).

Pennington, C.V.L., Evans, H.M. & Foster, C. (2009) Landslides of the area around Chesterfield, Geological Sheet 112. British Geological Survey, Open Report, OR/09/022.

Smith, E.G., Ryhs, G.H., and Eden, R.A. (1967) Geology of the Country around Chesterfield, Matlock and Mansfield (explanation of one-inch geological sheet 112, new series) Natural Environment Research Council, Institute of Geological Sciences incorporating the Geological Survey of Great Britain, the Museum of Practical Geology and Overseas Geological Surveys, London.

UNESCO, 2009. World Heritage and Buffer Zones. International Expert Meeting on World Heritage and Buffer Zones. Davos, Switzerland 11 – 14 March 2008. World Heritage papers 25. (Eds Oliver Martin & Giovanna Piatti). UNESCO World Heritage Centre.

Walsby, J. C. (2008). Geosure: a bridge between geology and decision making. From: D. G. E. Liverman, Pereira, C.P.G., Marker, B. Communicating environmental geoscience. London, Geological Society Special Publications. 305: 81-87.

Wang, L., Barkwith, A., Jackson, C., Ellis, M. (2012) SLiM : an improved soil moisture balance method to simulate runoff and potential groundwater recharge processes using spatio-temporal weather and catchment characteristics. [Lecture] In: 12th UK CARE Annual General Meeting, UK Chinese Association of Resources and Environment, Bristol, UK, 8 Sept 2012. (Unpublished) http://nora.nerc.ac.uk/id/eprint/19484

Appendix A

The Soil and Land-use based rainfall-runoff-recharge Model (SLiM)

The Soil and Landuse based rainfall-runoff and recharge Model (SLiM) model has been developed to objectively link both runoff and recharge processes to rainfall intensity, potential evapotranspiration, and catchment characteristics, such as soil type, land cover, topography, and baseflow index. It introduces the concept of soil moisture deficit (*SMD*) excess water and bypass runoff. *SMD* excess water is the amount of water added to the soil system when the soil store becomes full. SLiM calculates both recharge and runoff by relying on quantitative process based methods rather than expert judgement. It has been successfully adopted to estimate recharge at the catchment scale and national scale in several studies. The method can be easily integrated into other environmental models.

Hydrological processes in SLiM

There are many potential pathways that water can take through the system. Rainfall could, in part, be intercepted by plants, while the remaining rainfall reaches the ground surface and infiltrates the soil to increase *NSSS* and (or) reduce *SMD*. Soil water is extracted by plant roots for transpiration or drawn to the bare soil surface for evaporation. When soil moisture reaches field capacity (*SMD* becomes zero), water drains freely from the saturated soil, and the additional water added to the soil system, called the excess water of *SMD*, can flow laterally overland as runoff (including surface runoff and interflow) if a slope gradient exists towards adjacent locations, or percolate downwards through saturated soil as recharge. Runoff flows to nearby areas, called run-on, can join in the soil hydrological processes at the new location. If rainfall intensity is higher than the capability at which soil can absorb in a period of time, a part of rainfall quickly accumulates on the soil surface and becomes surface runoff without being able to enter the soil. This process is called bypass runoff and remains unaffected by the soil moisture conditions. SLiM explicitly derives both runoff and recharge based on the calculated *SMD* and other datasets, such as BFI and slope, instead of expert judgment.

The concept of *SMD* excess water

According to hydrological processes represented in SLiM, a drop of water that reaches soil surface will not generate runoff before *SMD* is reduced to zero (except during high intensity rainfall events). When soil becomes saturated, the water content above field capacity, which is defined as the *SMD* excess water, cannot be held against the gravitational forces and therefore drains through the soil to generate runoff and recharge. Döll et al. (2003) developed a similar algorithm of the soil hydrological processes to calculate *'total runoff'*, which is the sum of the recharge and runoff components, and split the recharge and runoff components using expert judgement; and the estimation of runoff and recharge is highly relying on people's experiences.

Base flow index (*BFI*) and slope were introduced into SLiM, allowing the *SMD* excess water to be proportioned between recharge and runoff. *BFI*, representing an average ratio of annual baseflow to annual river flow in a watershed or catchment, is strongly related to topography, soil, hydrogeological and precipitation characteristics and less influenced by the land-cover properties of a catchment (Haberlandt et al., 2001). We used *BFI* to split the *SMD* excess water into recharge, which might slowly enter rivers in the form of baseflow through the groundwater system, and runoff that flows overland:

$$RECH = E_{SMD} \cdot BFI \qquad \textbf{(1)}$$

$$Ro = E_{SMD} \cdot (1 - BFI) \qquad \textbf{(2)}$$

where E_{SMD} (mm) is the depth of *SMD* excess water when soil becomes free draining; $RECH$ (mm) is the depth of water that move downwards to recharge groundwater system; and Ro (mm) is the runoff calculated from E_{SMD}.

The topographic gradient is an important factor that controls runoff generation. In general, greater runoff is observed in areas with steeper slopes. As mentioned above, *BFI* is a long-term average ratio reflecting different catchment characteristics including average catchment slope. Therefore, the runoff and recharge calculated using equations 1 and 2 can be understood as the averages generated at the locations with an average slope in a study area. If a location has a higher than average slope, greater runoff and reduced recharge will be generated. In a flat area, where a zero slope gradient exists towards neighbouring locations, all *SMD* excess water becomes recharge and no runoff will be generated. Equation 2 can be further formulated as:

$$Ro = \frac{E_{SMD} \cdot (1 - BFI) \cdot Slp}{Slp_{mean}} \quad \text{when } Slp \le Slp_{mean} \qquad \textbf{(3)}$$

$$Ro = \frac{(Slp - Slp_{mean}) \cdot E_{SMD} \cdot BFI}{(90 - Slp_{mean})} + E_{SMD} \cdot (1 - BFI) \quad \text{when} \quad Slp_{mean} < Slp < 90 \qquad \textbf{(4)}$$

$$RECH = E_{SMD} - Ro \qquad (\textbf{5})$$

where Slp_{mean} (degree) is the average slope value in a catchment; and Slp (degree) is the slope value at a cell with the area.

Bypass runoff

Compared with a longer less intense rainfall, high intensity short duration rainfall is more likely to exceed the capacity of the soil to infiltrate water and generate more overland flow. Tani and Abe (1987) show that rainfall intensity and antecedent soil water storage in a forestry catchment affect the amount of runoff and, if the rainfall intensity is larger than a threshold (such as 100 mm day^{-1}), the increase in storm runoff is almost the same as the increase in rainfall, even with dry antecedent soil water conditions. Therefore, a rainfall intensity threshold is introduced in SLiM, to represent bypass runoff, where the amount of rainfall above this threshold becomes runoff. If the rainfall intensity is less than this threshold, the *SMD* excess water method is used for calculating runoff. The rainfall intensity threshold needs to be calibrated.

An improved algorithm for *SMD* calculation

TAW and *TEW* represent the maximum amount of water in the soil that is available for evapotranspiration, thus, *SMD* should not be higher than the weighted sum of *TAW* and *TEW* (representing the percentage of crop cover and bare soil) when simulating the soil water processes. An exception occurs following a harvest, when the crop is removed and the available soil water is reduced (*TAW* becomes zero for bare soil). However, the *SMD* calculation algorithm in Rushton's method does not take this situation into account. For example, when the antecedent *SMD* is less than *RAW* and there is no rainfall in the current time step, *AE* equals *PE*; however, if *PE* is larger than the amount of *TAW* minus *SMD* (the maximum soil water available for evapotranspiration), the newly calculated *SMD* will be larger than *TAW*. The improved *SMD* calculation algorithm in SLiM considers such a maximum soil water constraint.

Development of the SLiM code

Based on the methods described above, a C# code was developed. Using a GIS raster data structure, the code discretises the domain into uniform cells that contain distributed information, such as topography, rainfall and soil. SLiM uses a Digital Elevation Model (DEM) to derive information about the morphology of a land surface: slope gradient and aspect, flow directions, flow accumulation, river networks, and the watershed boundary using the Jenson (1991) method. The code has the option of automatically removing topographic depressions (ponds), which can hinder overland flow routing. Based on the derived flow accumulation, river and non-river cells can be defined using a flow accumulation threshold. For example, a threshold value of 50 allocates all cells with more than 50 upstream cells as river cells that together form a river network. A cell passes runoff to its eight neighbouring cells as a function of the slope values. The run-on process changes the distribution of overland water and hence that of soil water. Not all runoff will reach the main channel on the day it is generated and is stored on the land surface. The time lag and amount of runoff stored in overland and stream flow can be expressed using an exponential function of water travel time in one cell with a runoff lag coefficient (Neitsch et al., 2005):

$$Ro_{dis}^{t} = (Ro^{t} + Ro_{stor}^{t-1}) \cdot \left\{ 1 - \exp\left[\frac{-C_{lag}}{T} \right] \right\} \quad \textbf{(6)}$$

where Ro_{dis}^{t} (mm) is the depth of water (runoff or stream) discharged from one cell to its downstream neighbouring cell at the current time step; Ro^{t} (mm) is the depth of runoff generated at the current time step; Ro_{stor}^{t-1} (mm) is the depth of water stored at the cell from the previous time step; T (hour) is the water travel time from one cell to the next; and C_{lag} is the runoff lag coefficient. $1 - \exp\left[\frac{-C_{lag}}{T} \right]$ in equation 6 represents the fraction of the total available water in a cell that will be discharged to the next downstream cell. A higher C_{lag} value results in more water discharged to stream.

It worth noting that the spatial resolution of the rainfall datasets do not have to be the same as the model cell size, as the code can scale automatically between different spatial resolutions.

Model construction and calibration

Derwent catchment rainfall-runoff-recharge model

The distributed daily rainfall, land-cover LCM2000, DEM, the hydrology of soil types (HOST), and the river flow datasets are gathered from Centre for Ecology and Hydrology (CEH); the reference evapotranspiration dataset is from the Met Office Rainfall and Evaporation Calculation System (MORECS). The HOST dataset contains 29 soil classes of similar hydrological response and as well the BFI value for each class. River flow directions, river flow accumulations and a river network in the Derwent catchment (Fig. 1) were derived by the SLiM code after the depressions in DEM were filled automatically.

The study area is discretised spatially into over half a million square cells, each 200 m by 200 m, and temporally using a uniform time step of one day. All GIS raster datasets, including DEM, rainfall, land-cover, soil types and *BFI* were input into the SLiM code in an ASCII data format. The Institute of Hydrology low flow method for baseflow separation is used to generate surface flow components (called observed runoff in following sections) from the observed total river flow of river gauging stations (Fig. 1). The model calibration was undertaken based on visual inspection of hydrograph comparison. It shows that the simulated runoff matches the observed value adequately (e.g. Fig. 2 and 3).

National scale rainfall-runoff-recharge model for Great Britain

The national scale SLiM rainfall-runoff-recharge was constructed using the datasets of DEM, LCM2000, potential evapotranspiration, HOST, the thickness of low permeability superficial deposit. River flow from 87 gauging stations across Great Britain were used to calibrate the model.

8 The Nash-Sutcliffe efficiency NSE was adopted to calculate the goodness of fit between observed and modelled surface flow time series:

$$NSE = 1 - \frac{\sum_{i=1}^{N}(Vobs_i - Vsim_i)^2}{\sum_{i=1}^{N}(Vobs_i - \overline{Vobs})^2} \qquad \textbf{(7)}$$

where $Vobs_i$ is the observed surface flow at the i^{th} time step; $Vsim_i$ the simulated flow at the i^{th} time step; N is the total number of simulation time steps; and $\overline{Vobs}$ is the average value of observed flow in N simulation times.

After calibration, 86% of gauging stations have *NSE* > 0.5, which gives acceptable model performance. Fig. 4 and 5 show the examples of the comparison of modelled and observed hydrographs.

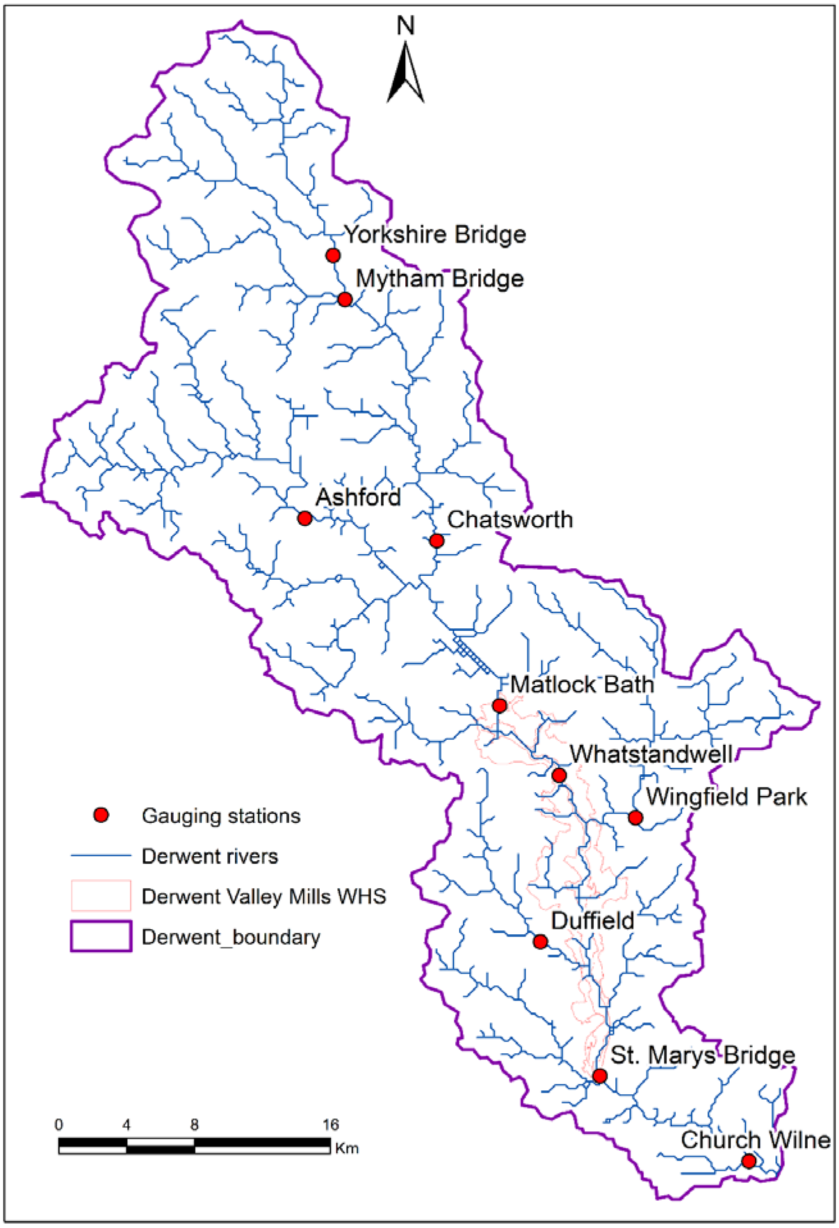

Fig.1 The Derwent catchment and its river gauging stations

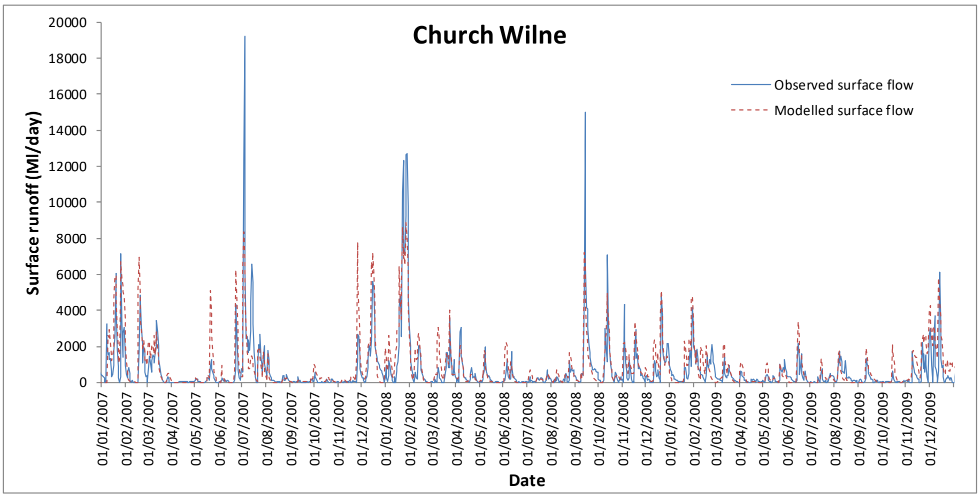

Fig.2 Comparison of simulated and observed daily runoff at Church Wilne

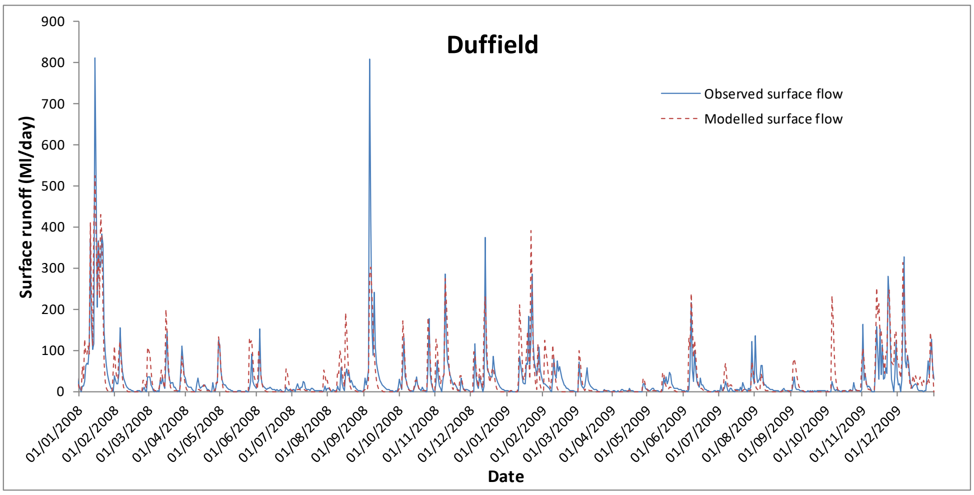

Fig.3 Comparison of simulated and observed daily runoff at Duffield

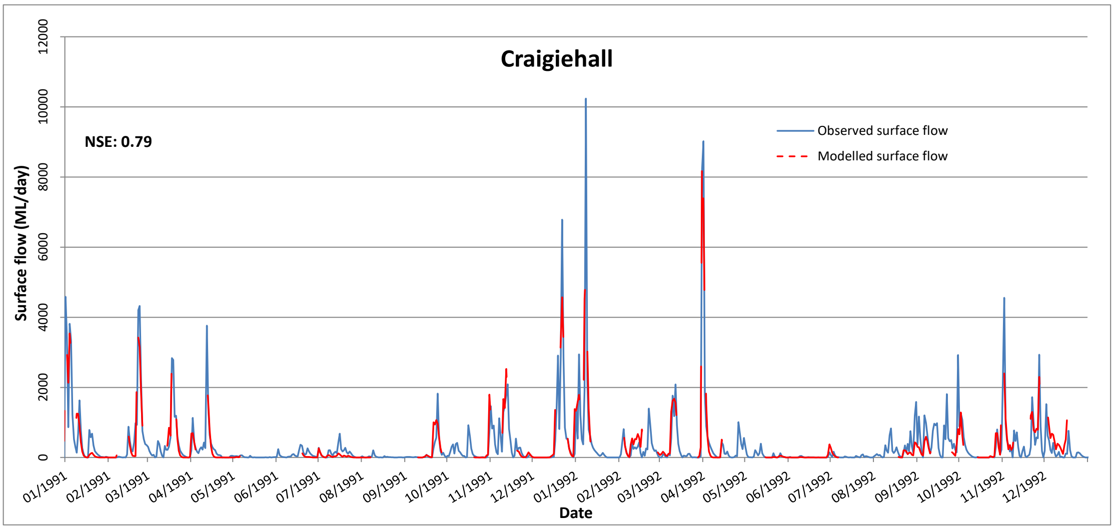

Fig.4 Comparison of simulated and observed daily runoff at Craigiehall

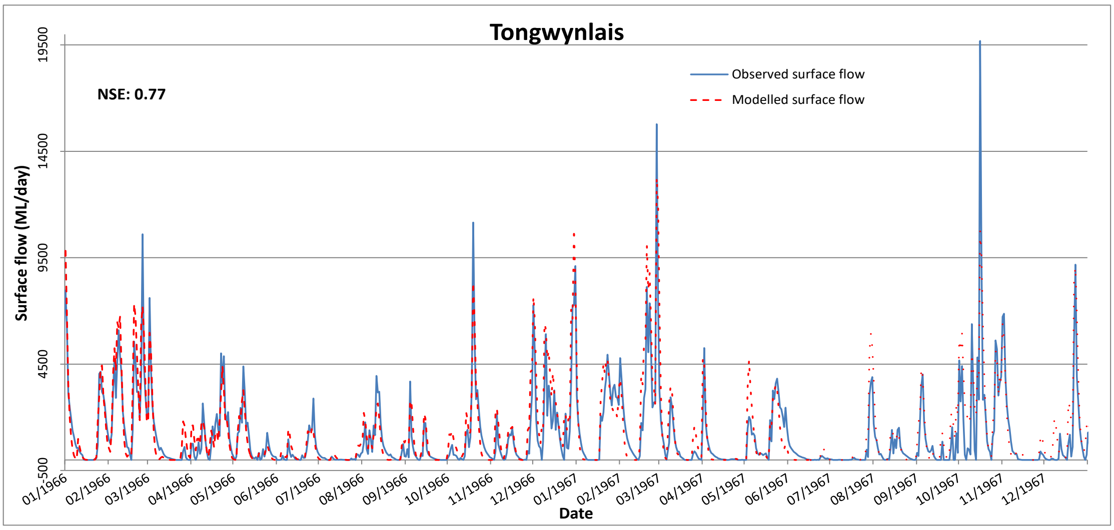

Fig.5 Comparison of simulated and observed daily runoff at Tongwynlais